

Solving the Extremely High Dead Time During  
Ultra-High-rate Gamma-ray Spectrometry Using  
a LaBr<sub>3</sub>(Ce) Detector

Solving the Extremely High Dead Time During  
Ultra-High-rate Gamma-ray Spectrometry Using  
a  $\text{LaBr}_3(\text{Ce})$  Detector

By: Tianyi Ren, BSc (Hons.)

A Thesis Submitted to the Department of Radiation Science and the School of Graduate  
Studies in Partial Fulfillment of the Requirements for the Degree Master of Science

McMaster University © Copyright by Tianyi Ren, September 2022

McMaster University MASTER OF SCIENCE (2022) Hamilton, Ontario (Radiation Science)

TITLE: Solving the Extremely High Dead Time During Ultra-High-rate Gamma-ray  
Spectrometry Using a  $\text{LaBr}_3(\text{Ce})$  Detector

AUTHOR: Tianyi Ren, BSc. (Hons.) (McMaster University)

SUPERVISOR: Dr. Soo Hyun Byun, Ph.D.

NUMBER OF PAGES: xii, 79

## Abstract

One of the main challenges during the ultra-high count rate gamma-ray spectrometry is the large dead time. Using a  $\text{LaBr}_3(\text{Ce})$  detector (TRT  $0.3 \mu\text{s}$ , TFT  $0.5 \mu\text{s}$ ), with an input count rate of  $4.8 \times 10^5$  cps, the dead time could be as high as 87% [1]. Such high dead time could significantly reduce the quality of the data collected as a considerable number of counts would be lost. Thus, this project aimed to reduce the dead time by modifying the detector system. Based on the setup used by previous research, the new system has its preamp, which is normally used for signal processing, removed. Experiments were made with calibration sources to optimize the new system. The calibration sources (Cs-137 and Co-60), Cs-137 resin sources, and Shephard Cs-137 sources were used to create different count rates, with the highest being  $1.22 \times 10^6$  cps, for measurements. Side-by-side measurements were performed with the setup with preamp and the one without preamp at various count rates. The analysis, which focused on the dead time and resolution, shows the setup without preamp would have much lower dead time, especially during ultra-high count rate measurements. The method was proved to be successful, for, at  $4.8 \times 10^5$  cps, the dead time decreased from 87% to 54%.

## **Acknowledgements**

Firstly, I would like to thank my supervisor, Dr. Soo Hyun Byun, for his guidance during my studies as an undergraduate and graduate student at McMaster University. His unparalleled abilities in both teaching and motivating helped me work through the difficulties throughout the research. Without his help and patience, this research would not be possible. I am extremely honored to have studied under his supervision.

I would also like to thank my committee members, Dr. Alan Chen and Dr. Jovica Atanackovic, for their advice and patience. Without their help, this project would not be where it is today.

I would like to thank my colleagues for their constant help throughout the years. Without them, the journey would never be as fun and memorable as it is.

Finally, I thank my family for their love and support. Without their encouragement, I would never be where I am today.

# Contents

Abstract.....	iv
Acknowledgements.....	v
List of Abbreviations.....	vii
List of Figures.....	viii
List of Tables .....	xi
1. Introduction.....	1
2. Gamma-ray Spectroscopy System.....	13
3. Optimization of the shaping parameters.....	21
4. Calibration Source and Resin Source Measurements.....	36
5. Shephard Cs-137 Sources Measurements.....	54
6. Conclusion.....	76
Reference.....	78

## List of Abbreviations

HV	High Voltage
HPG	Hyperpure Germanium
LaBr <sub>3</sub> (Ce)	Lanthanum Bromide, Cerium-doped
PMT	Photomultiplier Tube
ICR	Input Count Rate
TRT	Trapezoid Rise Time
TFT	Trapezoid Flat Top
Lsb	Least significant bit

## List of Figures

1.1	Picture of the $\text{LaBr}_3(\text{Ce})$ used for experiment	6
1.2	The pile up of the signal in preamp	10
2.1	Old setup for Gamma-ray measurements (With Preamplifier)	13
2.2	New setup for Gamma-ray measurements (Without Preamplifier)	14
2.3	Picture of setup with preamp	14
2.4	Picture of setup without preamp	15
2.5	$\text{LaBr}_3(\text{Ce})$ detector used for measurements (With Preamp)	16
2.6	Port for preamp unit connection	17
2.7	The Preamp unit and the connector on its back	18
2.8	Interface for the setup without preamp	18
2.9	HV power supply (C9525 by HAMAMATSU)	19
2.10	DT5724 Digitizer manufactured by CAEN	20
3.1	An input signal and its shaped pulse by the trapezoidal filter	22
3.2	COMPASS software with its control for shaping parameters	23
3.3	Setup for parameters optimization (without preamp)	24

3.4	Spectrum obtained from the calibration source	24
3.5	Spectrums for different HV options	28
3.6	Spectrums for different threshold options	31
3.7	Setup for calibration source measurements (with preamp)	32
3.8	Background spectrum obtained with preamp	34
3.9	Background spectrum obtained without preamp	34
4.1	Sample of the software running in wave mode	38
4.2	Source arrangement for resin source measurements	41
4.3	Sample spectrum for the measurements for resin source	42
4.4	Sample spectrum for the measurements for resin source	46
4.5	Measurements with different rates (with preamp)	49
4.6	Relation between resolution and input count rate	50
4.7	Relation between resolution and input count rate	52
5.1	Setup for the measurements with ion chamber	55
5.2	Setup for measurements with LaBr <sub>3</sub> (Ce) detector (with preamp)	55
5.3	Sample spectrum of the measurements obtained without preamp	57
5.4	Spectrum at various positions acquired without preamp	58

5.5	Spectrum with different voltages (without preamp)	60
5.6	Spectrum with different shaping parameters (without preamp)	62
5.7	Spectrum of the measurements for the setup with preamp	64
5.8	Spectrum at a different position (with preamp)	65
5.9	Sample spectrum at 1m position (with preamp)	66
5.10	Measurements with calibration sources (with preamp)	67
5.11	Spectrum at 1m position with new preamp power supply	69
5.12	Spectrum with different voltages settings at 1.5m (with preamp)	70
5.13	Spectrum with different Parameters at 1.5m (with preamp)	71

## List of Tables

3.1	Summary of results from shaping parameters optimization	25
3.2	Summary of results from different HV options	28
3.3	Summary of Min energy from different HV	29
3.4	Summary of Min energy from different threshold	31
3.5	Summary of resolution from our and Laranjeiro's work	33
3.6	Lowest energy on the spectrum (setup with preamp)	33
3.7	Maximum energy for each setup (based on background spectrum)	35
4.1	Summary of measurements from calibration sources	37
4.2	Summary of measurements with different modes	39
4.3	Summary of measurements with different setups (list mode)	40
4.4	Summary of measurements with different shaping parameters	43
4.5	Measurements with different thresholds (without preamp)	44
4.6	Measurements with different count rates (without preamp)	45
4.7	Measurements with different parameters (with preamp)	47
4.8	Measurements with different count rates (with preamp)	49

4.9	Measurements using CAEN preamp power supply	51
4.10	Measurements using two setups (with/without preamp)	53
5.1	Measurements at multiple positions (without preamp)	58
5.2	Our measurements and Laranjeiro's CANDU measurements	59
5.3	Measurements at various voltages (without preamp)	60
5.4	Measurements with different parameters (without preamp)	62
5.5	Measurements from ion chamber and P200	73
5.6	Dose rate from both ion chamber measurements and calculation	75

# Chapter 1

## Introduction

### 1.1 Motivation

Nowadays, nuclear power has become a major component of worlds' energies supply. Since 2020, Ontario has 60% of its power supply coming from nuclear reactor [21]. Since the last century, the call for green energy turned many interests into the nuclear industry. Furthermore, recent conflicts in Ukraine and the following increase in fossil fuel prices also promoted the introduction of nuclear energy. Discussions for the possibility of building or reopening reactor have arisen in Europe, as the needs for a cheap alternative energy supply increase.

Despite the attractive aspects of nuclear energy, the potential harm from ionizing radiation is real and present. Both deterministic and stochastic effects could be caused by exposure and cause series of health issues. In Canada, Canada Nuclear Safety Commission (CNSC) regulates and supervises the nuclear industry and promote its safe operations. Thanks to strict regulation and effective monitoring system, in the past forty years, no members of the public in Canada became the victim of radiological release. But to maintain or even further improve the protection, more accurate dose information would be needed.

There are challenges in actual practices, as the ultra-high-count measurements in reactor would have limited reliabilities. Generally, the detector used for such measurements would be perfectly capable of performing accurate measurements at lower count rate. However, at higher count rate the dead time issue would inevitably affect the quality of the results [1].

Dead time, which is the summation of all the processing time, would limit the processing rate of the system, as the next event would not enter processing until the previous one has finished. In other words, at ultra-high-count rate, the combination of high-count rate and larger overall dead time would lead to loses of considerable amount of data. Taking one measurement from our experiments as example, the 45% dead time would mean roughly 45% of the input signals would be lost during the process. This issue would only become more severe once the count rates increase.

Furthermore, certain components of the system would also limit its overall performance at ultra-high-count rate measurements. One of such examples would be the preamp attached to the detector. The voltage applied at the preamp could affected the highest allowed count rates. Its design would also limit its ability to process the high-rate input signals. Thus, a new detector or a new system arrangement would be needed.

In the last two decades, with the advancements in material science and engineering, it has been possible to create and apply newer detectors into practice. Research on whether these new detectors can be used for real-life measurements has been conducted

worldwide. One such example is the high purity germanium (HPGe) detector for gamma-ray spectroscopy at high count rates made by R.J. Cooper, et al [2]. The count rate they measured was around  $1 \times 10^5$  cps [2]. Cooper tried to balance the efficiency and count rate in his research by building a prototype HPG detector. The result was promising as the detector can provide satisfactory resolution at a high-count rate. However, as the HPG detector would require a cooling system containing liquid nitrogen, it is not suitable for portable use. Thus, an alternative detector would be needed.

Scintillation detectors, especially the  $\text{LaBr}_3(\text{Ce})$ , have the capability to process a high-count rate while having portable designs [6]. Research has been conducted on whether the Scintillation detectors can be used for high count rate gamma-ray spectrometry. In High count rate  $\gamma$ -ray spectroscopy with  $\text{LaBr}_3(\text{Ce})$ : Ce scintillation detectors by B, Löher, et al, they proved the  $\text{LaBr}_3(\text{Ce})$  detector can operate with a good resolution even with a count rate of 14MHz [3]. In another research done by Nocente. M, et al. they measured the gamma-ray emitted from fusion plasma and showed that  $\text{LaBr}_3(\text{Ce})$  could perform gamma-ray spectrometry with a count rate up to 4MHz [4]. Each research shows the  $\text{LaBr}_3(\text{Ce})$  detector is capable of high-rate measurements. The next step was to prove the  $\text{LaBr}_3(\text{Ce})$  detector could provide reliable data in reactor environments.

One such work is done by A. Laranjeriro, which focuses on the characterization and optimization of a  $\text{LaBr}_3(\text{Ce})$  detector for the ultra-high-count rate spectrometry at CANDU reactors [1]. In his project, a  $\text{LaBr}_3(\text{Ce})$  detector was used for measurements and provided

good results. However, despite the success, certain issues arose. While the system would function fairly well in a low-count-rate environment, in a CANDU reactor where the count rates are much higher, the system would have super high dead time, affecting the measurements' reliability. One such example would be at  $5.4 \times 10^7$  cps input count rate; the dead time was 91% [1].

Thus, in this research, the main goal is to find a method to overcome the high dead time challenge that was encountered by A. Laranjeriro at high count rates. In order to do so, we made a major change for the pulse processing system by removing the preamplifier. Overall, this research contains four parts. Firstly, we began with the assembly and optimization of the new system in terms of resolution and dead time. Secondly, with the system now optimized, we performed the comparison between the new and old setup at low count-rate environment. Thirdly, we repeated the similar comparison at higher-count rate environment. Finally, we used the Shephard source in McMaster University to produce ultra-high-count rate environments and conduct measurements. The goal is to find out if the new setup would have better performance.

## **1.2 Overview**

### *1.2.1 Work by A. Laranjeriro*

In his work, A. Laranjeriro tried to use the  $\text{LaBr}_3(\text{Ce})$  detector for gamma-ray spectrometry [1]. By using different radiation sources, series of testing measurements helped him to

choose the most ideal shaping parameters. Also, the MCNP modeling showed the detector's sensitivity to the angles. Finally, the measurements at different CANDU reactors showed the efficiency of the  $\text{LaBr}_3(\text{Ce})$  detector in ultra-high-count rate measurements. His works proved the  $\text{LaBr}_3(\text{Ce})$  detector can be used for gamma-ray spectrometry with various measurements while having good resolutions. His setup and methods became the groundwork of this project.

However, Laranjeriro pointed out in his work that the dead time issue would be a major problem in ultra-high-count rate measurements [1]. As the count rate increased, the dead time also increased accordingly. During the CANDU measurements, as the count rate reached  $5.4 \times 10^7$  cps, the dead time would increase to 91% [1]. Even at slightly lower count rate, the dead time would still be relatively high. Such high dead time could cause serious issues, as considerable amount of data would be lost due to the limited capacity of the system. Laranjeriro pointed out the future research should be more focusing on solving the dead time issue [20]. And that became the seed of this project.

### *1.2.2 Scintillation Detector*

Scintillation detector is among one of the oldest type of detectors. Its capability of producing visible light as output make it easy to operate and provide easy to read results. Nowadays, similar to other types of detectors, scintillation detector would have its output signals converted into voltage for easier processing.



*Figure 1.1: Picture of the LaBr<sub>3</sub>(Ce) used for experiment*

Scintillation detector can be divided into organic, and inorganic based on the type of crystal they used. Despite the difference in the type of crystals, scintillation detector has similar structure: a crystal for radiation interaction and a PMT(Photomultiplier) tube for electron signal generation. The detector used for the research is a LaBr<sub>3</sub>(Ce) detector which is a typical inorganic scintillation detector.

The first part of the detector is always the crystal. In pure crystal, only certain energy bands can present, and the energy that present would determinate the range of the energy. In reality, small amount of impurity would also be added to the pure crystal and acted as activators. These activators would change the energy structure and help detector creating signal in visible light range.

During the measurements, incoming radiation would enter the detector and interact with the crystal. During this process, the photons and their energy would be absorbed by the

in-valence band electrons which then become excited. Excited electrons would eventually return to the ground state by emitting their additional energies in the form of photons. During this process, the emission spectrum would be shifted to longer wavelength which would generate photons in the visible range. It would be the end of the process in traditional scintillation detector, but the modern detector has one more component: PMT tube.

The photons emitted from the crystal would enter the PMT tube where they would be converted into electrical signal. Incoming photons would first interact and be absorbed by the photocathode material. This process would generate low-energy electron with average energy of 1eV [5]. Due to the loss of the energy during the process, generated electrons would be less than the incident photons. To solve this issue, electron multiplication was introduced.

In experiment, a high voltage has to be applied on the PMT. The high voltage is used for the acceleration of low-energy electrons. The electrons would be accelerated and have much larger kinetic energy when they eventually hit the electrode. The deposited kinetic energy would then create secondary electrons. In the PMT tube, chains of such multiplication would happen and create hundreds of secondary of electrons from one incident low-energy electron. This would then provide sufficient signals for further processing.

### *1.2.3 Dead Time*

As detector generate an output signal, this signal has to go through series of processes before it is finally converted into pulse height spectrums. Firstly, it has to go through the digitizer where the signal would be shaped and amplified, and then through the data collecting laptop where the software would collect analysed data and form a pulse height spectrum. Depend on the setup, there would be more components the signals have to go through.

All those processes would take time to complete, and the next pulse cannot be processed before the current pulse is processed. The time between the two events is called dead time. In other words, dead time is the summation of all the processing time of each component in the system. Dead time can be presented either in second or in percentages of the real time and the later is more widely used.

Although small dead times may not affect the data too much, a high dead time could lead to misleading results. One of such examples can be taken from the actual measurements in this project. During one five-minute measurement, due to the high-count rate, the dead time was 49.67%. The high dead time cause serious issue as the input counts were  $1.38 \times 10^8$  and the output counts were only  $6.94 \times 10^7$ . About half of the input counts were lost due to the dead time. In Laranjeiro's work, the dead time could be extremely high during the ultra-high-count rate measurements. The highest recorded dead time from his

work is 91% [1] suggesting that considerable numbers of counts would be lost during the process.

### **1.3 Solving the dead time problem**

The main goal for this project is to reduce the high dead time during ultra-high-count rate measurements. Based on the nature of the dead time, one possible approach would be to remove certain component from the setup if possible.

The setup for this project is based on the setup used by Laranjeiro in his work [1]. The base setup is simple and contains several components: LaBr<sub>3</sub>(Ce) detector, preamplifier unit, high voltage supply, preamplifier power supply, digitizer and data collecting laptop. Among all the components, only one part can be removed: preamplifier.

Preamplifier, or in short preamp, is usually the first component after the detector. As the name suggests, the preamp should be placed before the amplifier. The main function for the preamp is to act as an interface between the detector and following pulse processing components. But it also slightly amplifies the signals. It would extract and collect the signal coming from the detector while trying to maintain a good signal-to-noise ratio.

In actual operation, incoming charges from the detector would be collected by the capacitor inside the preamp, and as the voltage in the capacitor becomes high enough a step change would then happen. After the step change, it will also take considerable

amount of time for it to restore to the baseline. All these processes would take time, and as the count rate increase the total processing time would also increase. Thus, the dead time would be higher.

Another limitation of the preamp in high-count rate measurement is also caused by the long decay time. Due to the long decay time, the next signal could arrive before the previous one return to the baseline. Thus, the next signal would ride on the previous one and signal height would increase. This pattern would continue as more and more pulses enter the preamp.

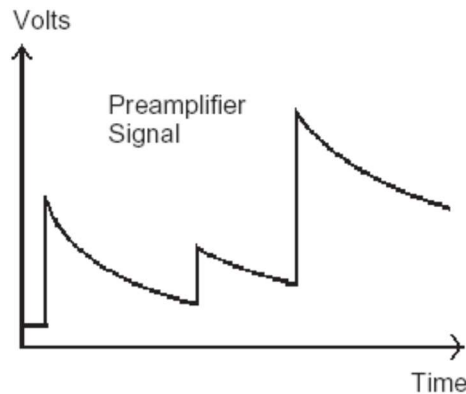


*Figure 1.2: The pile up of the signal in preamp*

At lower count-rate measurements, the pile up would not be an issue as the most important information is the rising edge of the signal which would not be affected by the pile up. The following pulse analysis system is also capable of extracting the signal from the pile up. However, at higher count rate, situation would be different. As the count rate increases, the pile up would also increase which means the signal would be further and

further away from the baseline. Because the maximum voltage provided by the preamp power supply is limited, once the signal height reaches the limit, the preamp would become saturated and unable to produce further output. In other words, the capacity of the preamp power supply would limit the maximum allowable count rate the system can process. This is a major issue in ultra-high count rate measurements.

Given the limitations of the preamp, in this project we tried to remove this component. By doing comparison between the new and old setups, we tried to prove the dead time can be decrease by using this new design. However, as the preamp could increase the signal to noise ratio, removing the module may cause the resolutions of the pulse height spectrums to degrade.

#### **1.4 Thesis Outline**

This thesis contained six chapter which covered all the aspects of this project. Chapter 1 included the introduction and motivation of this project, alongside with some basic information of the detector and dead time. Chapter 2 showed the overview of the systems used in this project and the individual components it contained. In chapter 3, we discussed how we managed to obtain the most ideal shaping parameters by using series of measurements. In the following chapter 4, we made comparisons between the two setups (with/without preamp) at different count rates. Continuing the comparisons in chapter 4, in chapter 5 we once again performed the similar measurements only with a

much stronger radiation source. In the end, chapter 6 concluded the project with a short overview.

## Chapter 2

### Gamma-ray Spectroscopy System

#### 2.1 Overview

In this project we used a  $\text{LaBr}_3(\text{Ce})$  detector for Gamma-ray measurements. In terms of the setup, we have two slightly different arrangements which correspond to A. Laranjeiro's old setup and our new setup [1]. The overall designs are rather similar and share most of the equipment.

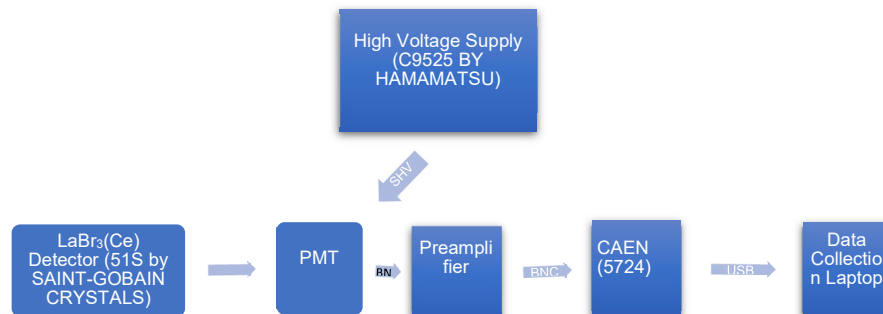


Figure 2.1: Old setup for Gamma-ray measurements (With Preampfier)

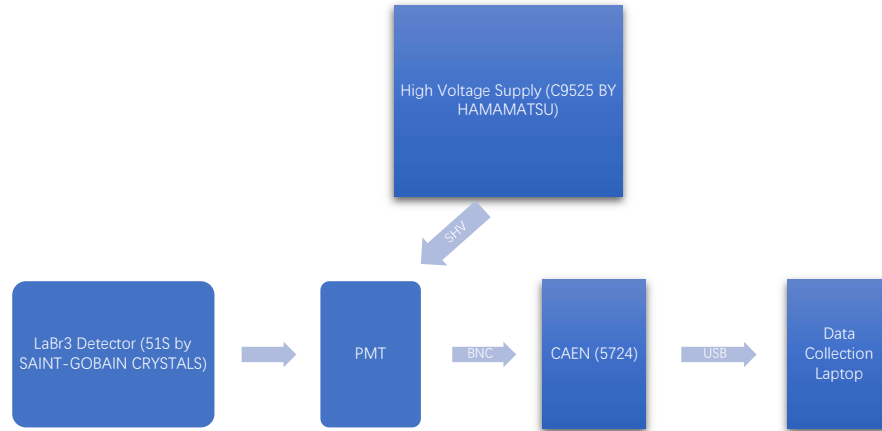


Figure 2.2: New setup for Gamma-ray measurements (Without Preamplifier)

Both setups contain a LaBr<sub>3</sub>(Ce) detector, a high voltage supply, a digitizer and a data collection laptop. The main difference is that the preamp and preamp power were removed from the new setup. In the following sections, we discuss each individual component in this setup.

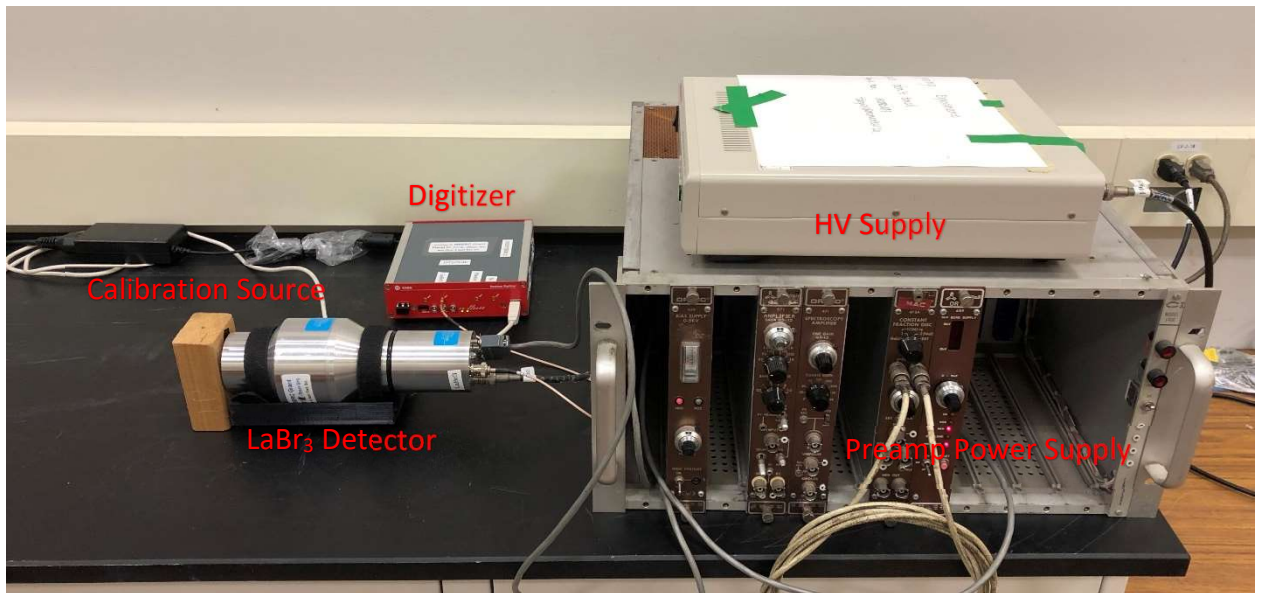
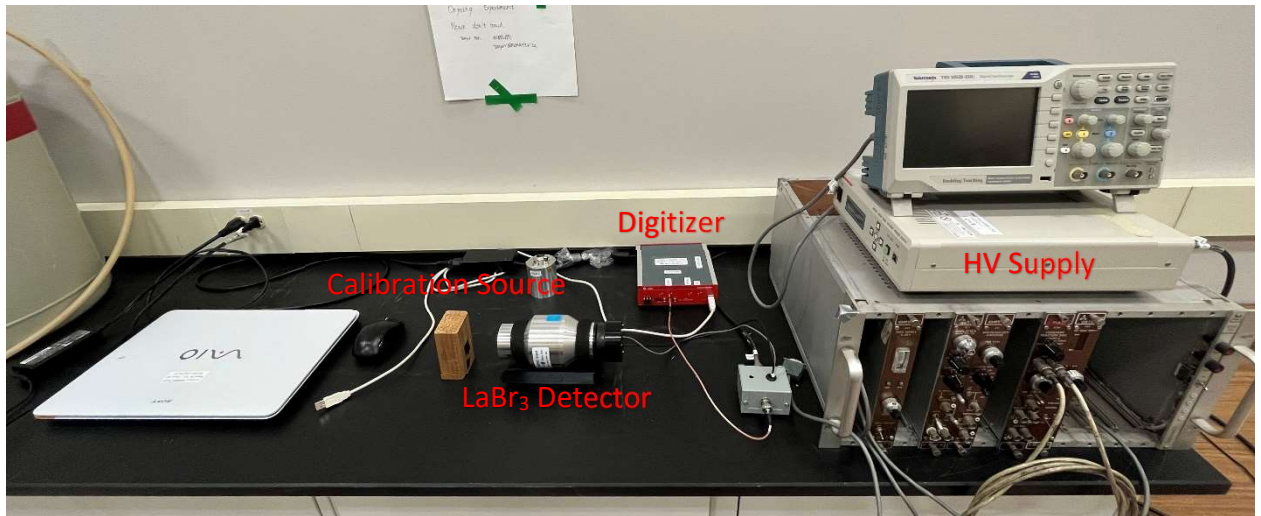


Figure 2.3: Picture of setup with preamp



*Figure 2.4: Picture of setup without preamp*

## 2.2 LaBr<sub>3</sub>(Ce) Detector

The LaBr<sub>3</sub>(Ce) used in this project is a model BrillanCe™ 380 detector manufactured by Saint-Gobain company. The unique characteristic of this detector is that the PMT tube itself is integrated with the detector. A preamp unit contains ports for preamp power supply, signal output and high voltage supply can be attached to the detector. Because only one connector is located at the end, if the preamp unit was not used, an alternative connecting unit would be needed. The detector is depicted in figure 2.5:



*Figure 2.5: LaBr<sub>3</sub>(Ce) detector used for measurements (With Preamp unit attached)*

This LaBr<sub>3</sub>(Ce) contains a 50.08 × 50.08 mm Lanthanum Bromide crystal with a thickness of 38.84mm [10]. According to the manufacturer, this detector has a light yield of 63 photons/keV which is much higher than the 38 photons/keV of a NaI detector [8]. Thus, more photons would be emitted. In addition, the primary decay time for this detector is also very short. With a decay time of 16ns, the detector is suitable for high-count rate measurements [9]. Finally, the LaBr<sub>3</sub>(Ce) performance manual stated that the detector has better resolution with energies above 100keV. The manual also stated the average resolution of 662keV peak would be 2.6% [9]. However, we were not able to achieve this value in actual measurements.

At the end of the detector, as shown in figure 2.6, there is a port for preamp. For there are no other ports, extra units would be needed to connect the digitizer and high voltage supply with the detector.



*Figure 2.6: Port for preamp unit connection*

For the setup with preamp, we attached the preamp unit with the detector. As showed in figure 2.7, the unit contains the nine-pin port for the preamp power supply, a BNC port for signal output and a SHV port for high voltage supply.

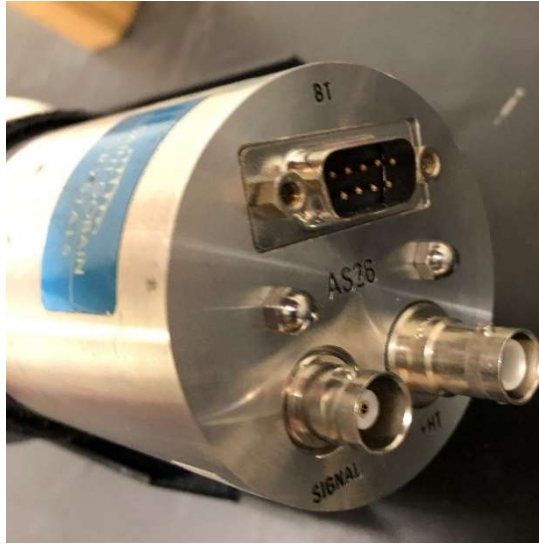


*Figure 2.7: The Preamp unit and the connector on its back*

For the setup without preamp, we used a special unit as the interface between the detector and other instruments as showed in picture 2.8. The unit contains a black connector for the detector and a small grey for the high voltage supply and digitizer.



*Figure 2.8: Interface for the setup without preamp*

## 2.3 Accessories

### 2.3.1 High Voltage supply

The high voltage supply used in this project is a C9525 HV power supply made by HAMAMATSU. It has a voltage output range of  $\pm 2000\text{V}$  and maximum output current of  $1.8\text{mA}$  [15]. One SHV port is available for the connection with the detector. In term of the control, the HV supply requires manual control and has the option to change voltage at single digit.



Figure 2.9: HV power supply (C9525 by HAMAMATSU)

### 2.3.2 Pulse Processing System

A DT5724 digitizer made by CAEN was used for this project. This digitizer has a full-scale range of  $2.55\text{Vpp}$  [12]. Four channels, 14bit system and a sampling speed of  $100\text{MS/s}$  on each channel enable it to work in high-count rate environments [11]. The system is controlled by the CAEN MC<sup>2</sup> software on the data collection laptop.

The signal from the detector (or from preamp, depends on the setup) first enters the digitizer. Then system performs Digital Pulse Processing for the Pulse Height Analysis (DPP-PHA). The input signal is digitized and processed using a trapezoid shape filter.

Pulse shaping parameters (input rise time, trapezoid rise time, etc.) can be changed by using the MC<sup>2</sup> software. The software can also show real-time pulse shape for shaping parameters adjustment. The dead time information can also be easily obtained through the use of the information function on the software. Various functions including detailed peak information and both input and output count rate enable quick access to much needed data. In addition to these features above, two modes (list mode and wave mode) provide different options for the data analysis. The digitizer is depicted in figure 2.10.



*Figure 2.10: DT5724 Digitizer manufactured by CAEN*

## Chapter 3

### Optimization of the Shaping Parameters

#### 3.1 Overview

Before the input signal can be observed on the laptop, signals first enter the digitizer and are processed with a trapezoid filter. The choice of the shaping parameters is critical to achieving both good accuracy and low dead time.

In this project, two setups require different shaping parameters as the component in use differs. For the setup with preamp, as the goal is to reproduce A. Laranjeiro's measurements for comparison, the shaping parameters were based on his settings. For the setup without preamp, we chose the parameters based on the standard approach, which is illustrated below.

First, the input signal must be properly collected before entering the next step. The input signal has two essential properties: rise time and exponential decay time. Among these two quantities, the rise time is more critical for it could determine if the input signal can be correctly collected. Figure 3.1 shows that it takes time for one signal to reach its maximum. The allowed time duration for build-up is controlled by the rise time. If the rise time is too short, then the maximum would not be reached, which would decrease the accuracy. However, long rise time would be unnecessary, and it also increases the dead time of the system.

During the experiment, the rise time was chosen by taking the average time it took for the signal to increase from baseline to the maximum. The following measurements further finalized this value. After the input signal is collected, a trapezoid filter is applied. Two important parameters control the filter: trapezoid rise time and trapezoid flattop. Figure 3.1 and figure 3.2 show examples of the waveform and parameters control interface. COMPASS software provides easy access to real-time waveform information and shaping parameters like the trapezoidal rise time. In the following sections, series of experiments were conducted in order to find the ideal trapezoid rise time and trapezoid flattop.

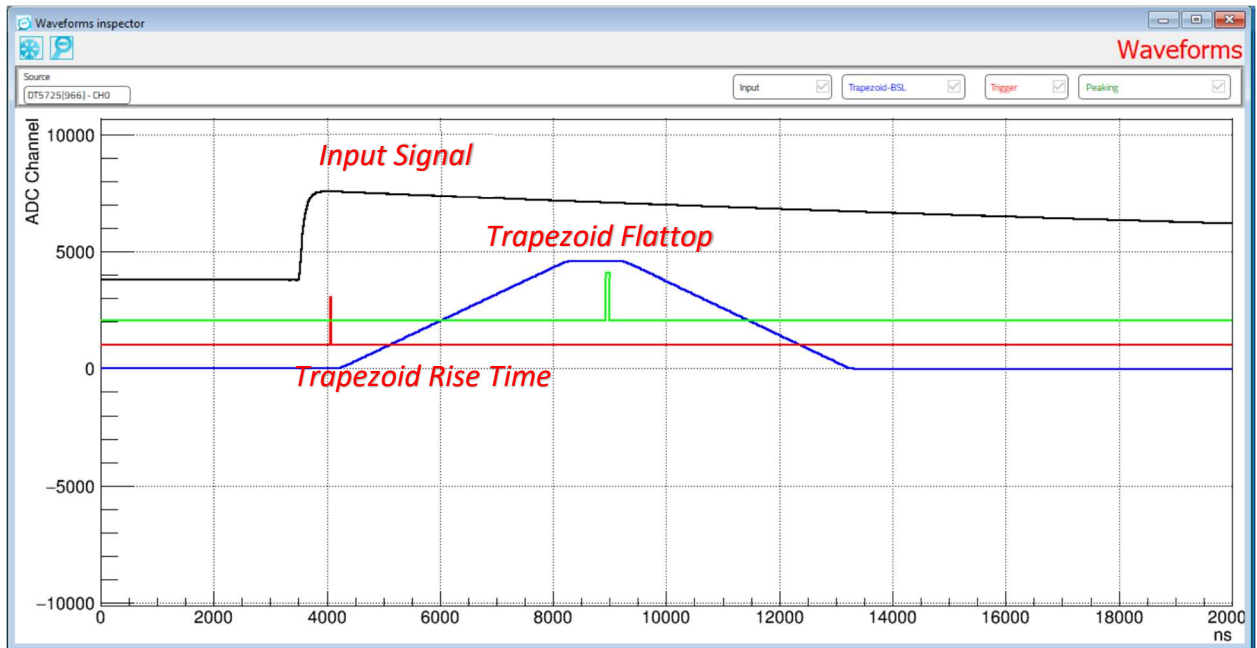


*Figure 3.1: An example of an input signal and its shaped pulse by the trapezoidal filter observed by the CAEN COMPASS software*

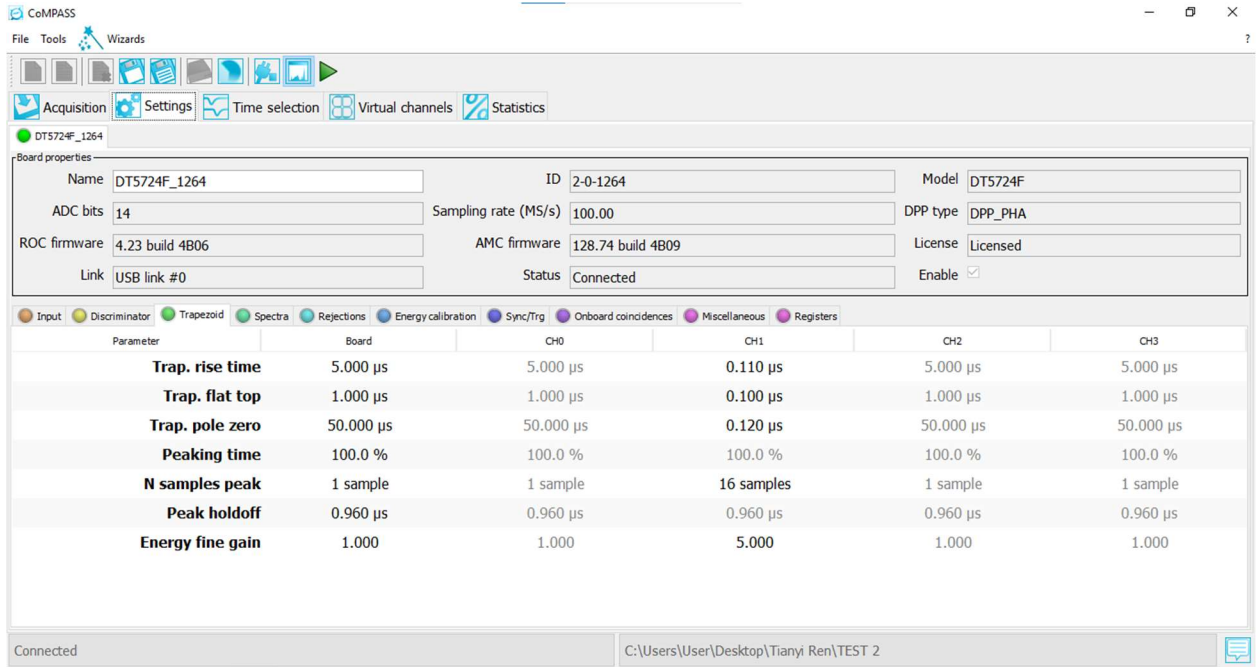


Figure 3.2: CoMPASS software with its control for shaping parameters

### 3.2 Measurements with calibration sources (without preamp)

In this section, a series of measurements were performed by using the calibration sources in the CAVE lab. The Cs-137 source was placed 15cm away from the detector, while the Co-60 source was placed in front of the detector. Equipment was arranged in the same order as the block diagram in the previous chapter. Figure 3.3 and figure 3.4 show the experiment setup and a sample spectrum:

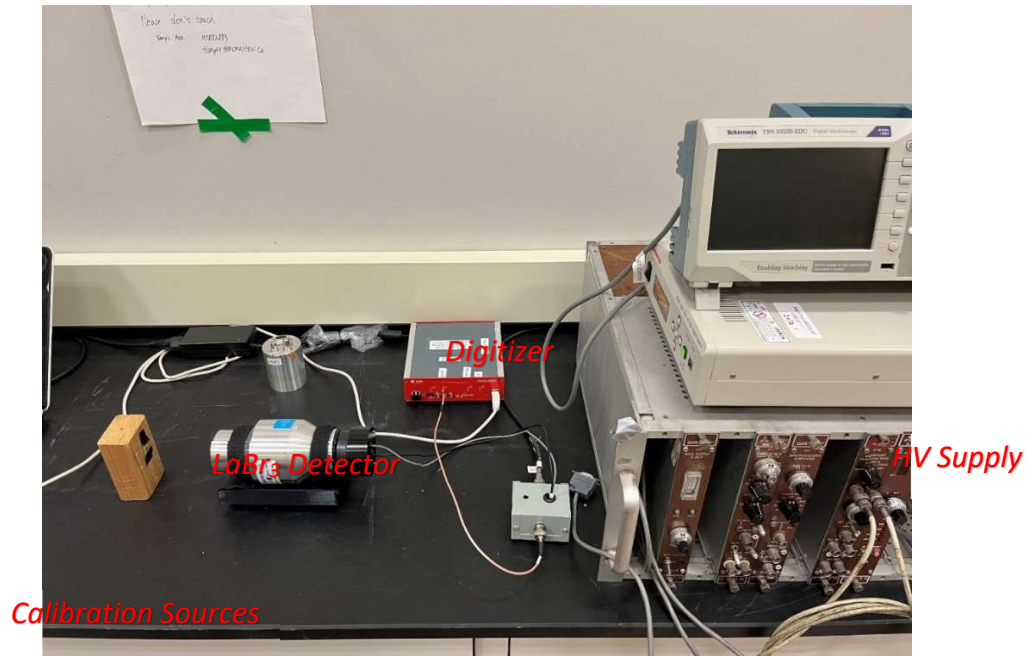


Figure 3.3: Experiment setup for pulse processing parameters optimization (setup without preamp)

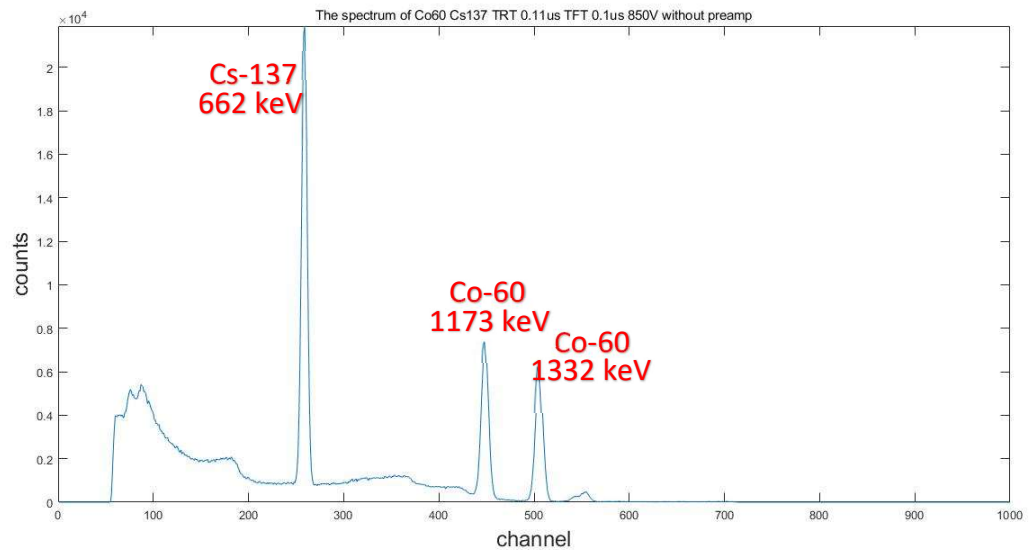


Figure 3.4: Spectrum obtained from the calibration source (setup without preamp, Trapezoid rise time 0.11  $\mu$ s, Trapezoid flattop 0.1  $\mu$ s)

Several sets of trapezoid rise time and trapezoid flattop combinations were selected and used for measurements, while the other parameters were kept the same. The analysis focused on the energy resolution, and dead time. FWHM, which is the full width of half maximum, when combined with peak centroid, can be used to calculate the resolution.

$$Resolution (\%) = \frac{FWHM}{Peak\ Centroid} \quad 3.1$$

Table 3.1 summarizes the results taken with different shaping parameters. It shows that different trapezoid rise time, and trapezoid flattop combinations would affect the resolution. If the parameters are too small, the resolution is larger. Thus, larger rise time and flattop are generally preferred since they provide better resolution. However, a larger rise time could increase the overall dead time. Furthermore, longer rise time and flattop could potentially lead to more pile-up, especially during the ultra-high count rate measurements. In conclusion, the ideal combination would be the one with better resolution, and relatively short trapezoid rise time and flattop.

*Table 3.1: Summary of results from shaping parameters optimization (setup without preamp)  
with input count rate around 1550cps*

TRT ( $\mu$ s)	TFT ( $\mu$ s)		Resolution (%)	Dead time (%)
0.08	0.08	Cs-137	5.22	1.66
		Co-60	4.86	1.66
			4.90	1.66
0.09	0.09	Cs-137	3.50	2.05
		Co-60	2.70	2.05

			2.79	2.05
0.10	0.10	Cs-137	2.72	1.64
		Co-60	1.80	1.64
			1.80	1.64
0.11	0.10	Cs-137	2.78	1.74
		Co-60	1.83	1.74
			0.81	1.74
0.12	0.10	Cs-137	2.81	1.71
		Co-60	1.85	1.71
			1.85	1.71

Compared with other combinations, the TRT 0.1 $\mu$ s and TFT 0.1 $\mu$ s combination appeared to have better resolution than others while having a good dead time. However, it is worth noting that according to the manufacturer, the detector can have a resolution up to 2.2% for 662keV peak [9]. From table 3.1, the best resolution obtained was 2.7% which was larger than this value. Hence, further optimizations are needed.

### 3.3 Finding the missing low channel information

During the measurements from the previous section, one issue appeared. Different from the measurements with the old setup (with preamp), the new setup (without preamp) generates spectrum with some low channel information appeared to be missing. From A. Laranjeiro's work, the smallest energy peak that appeared in reactor measurements is Xe-133 (81keV) [1]. Although the lowest energy peak actual presented in the measurements was Sb-125 (427keV) as the Xe-133 peaks may be too short [1]. It would be more desirable for us to be able to cover the Xe-133 energy peak at 81keV. With the current setting, the

81keV peak is not covered by the spectrum. Another issue was that with the settings, the spectrum would begin at channel 65, which means lots of information would be missing. Thus, certain parameters had to be adjusted.

Two options were available: firstly, changing the thresholds so more signals, especially the low energy signal, would be accepted. This would also extend the lower boundary of the spectrum and provide more low-energy information. Secondly, increasing the high voltage applied to the detector. The goal was to increase the number of electrons generated by the low-energy photons by increasing the voltage applied to the PMT tube.

### *3.3.1 Changing the HV*

Experiments began with different HV options. In a series of measurements, all shaping parameters were kept constant with only HV increase with a step width of 10V. The trapezoid rise time and trapezoid flattop was chosen from the previous section (0.1 $\mu$ s and 0.1 $\mu$ s).

Figure 3.5 and table 3.2 show the results obtained with different HV values. It can be concluded that by increasing the HV, more low channel information can be included in the spectrum. Table 3.3 shows the minimum energy from each set of measurements. It can be concluded that with the current setting, even with 900V HV, the Xe-133 peak (81keV) could be missing. Given that the Sb-125 (427keV), the isotope of interest with the lowest peak energy, can be covered by the 850V settings, 133keV would be an acceptable

lower boundary. Another issue was that the lower limit remained at 65 channels. Hence, changing the voltage may not be an ideal option.

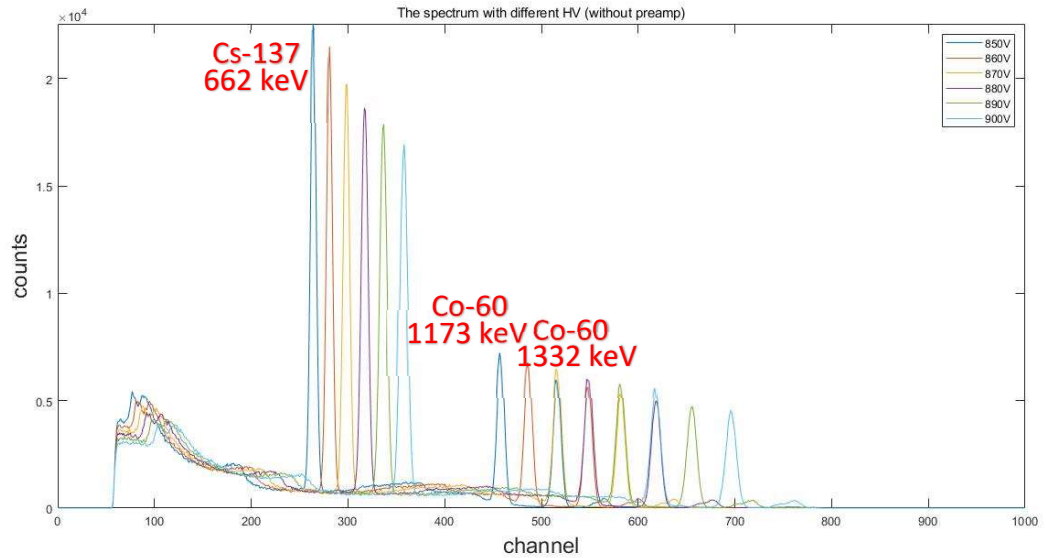


Figure 3.5: Spectrums for different HV options (Setup without preamp, Trapezoid rise time  $0.1\mu\text{s}$ , Trapezoid flattop  $0.1\mu\text{s}$ )

Table 3.2: Summary of results from different HV options (setup without preamp)

Voltage (V)	ICR (cps)		Resolution (%)	Dead time (%)
850	1609.56	Cs-137	2.65	1.85
		Co-60	1.97	1.85
	1631.71		1.74	1.85
860		Cs-137	2.85	1.86
		Co-60	2.05	1.86
	1609.25		1.82	1.86
870		Cs-137	2.68	1.94
		Co-60	1.93	1.94
	1629.88		1.72	1.94
880		Cs-137	2.84	1.92
		Co-60	1.83	1.92

	1648.38		1.78	1.92
890		Cs-137	2.67	2.04
		Co-60	1.89	2.04
	1665.01		1.68	2.04
900		Cs-137	2.23	2.14
		Co-60	1.94	2.14
			1.72	2.14

*Table 3.3: Summary of Min energy from different HV*

Voltage (V)	Min Energy (keV)
850	133
860	122
870	110
880	101
890	92
900	83

### *3.3.2 Changing the threshold*

The threshold in the COMPASS software functions as the name indicates: cut off the unqualified signal. Only the signal high enough would be accepted and then processed by the system. Thus, the noise would be filtered out and processing time shortened.

The threshold setting previously used was based on the parameters for the setup with preamp. However, 30lsb (least significant bit) setting appeared to be too high as the input signals from the setup without preamp are lower. The spectrum began at channel 65, and no information can be found at the lower channel. Hence, with 30lsb threshold, more

signals would be lost. The threshold had to be lower so the lower boundary could be extended to the left.

The main issue was how low the threshold should be moved. In a series of experiments, we tried four different thresholds: 30lsb, 25lsb, 20lsb, 15lsb. It was expected that the spectrum would overlap with each other, however, the spectrum with lower threshold should be able to cover lower channels.

Figure 3.6 shows the spectrums taken with different threshold settings. Table 3.4 shows the different thresholds and their corresponding lowest energies. Based on the data collected, both 15lsb and 20lsb enable the spectrum to cover the Xe-133 peak. Considering the dead time would be higher with a lower threshold due to the presence of more signals, it would be better to set the threshold at 20lsb. Also, we changed the channel gain from 2048 to 4096 for the following measurements. By doing so, we were able to obtain wider peaks for quicker and easier analysis.

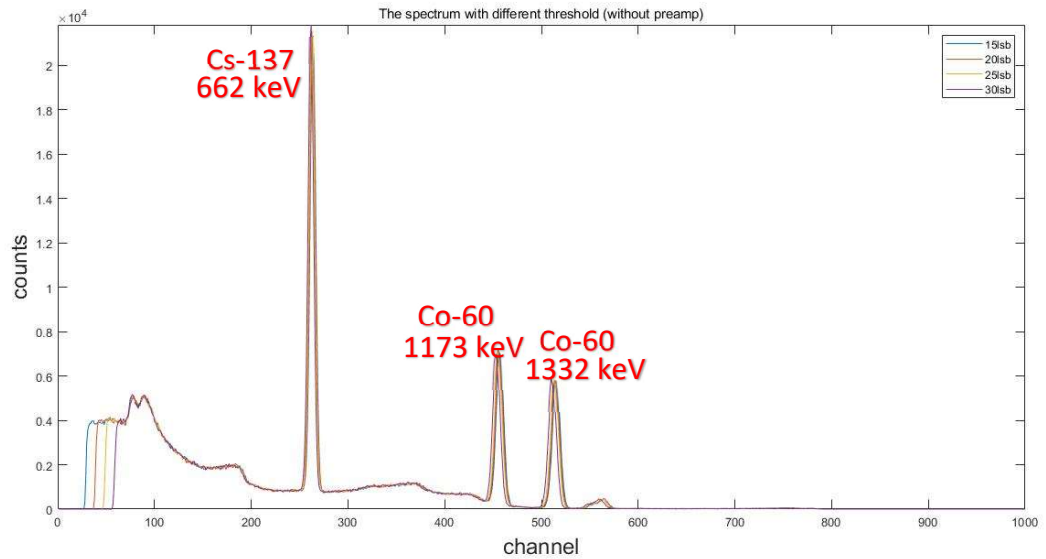


Figure 3.6: Spectrums for different threshold options (Setup without preamp, Trapezoid rise time  $0.1\mu\text{s}$ , Trapezoid flattop  $0.1\mu\text{s}$ )

Table 3.4: Summary of Min energy from different threshold

Threshold (lsb)	Lowest Channel	Lowest Energy (keV)
15	30	35
20	40	60
25	50	85
30	60	110

### 3.4 Measurements with calibration sources (with preamp)

For the setup with preamp, we used the same shaping parameters as in A. Laranjeiro's work [1]. As the detector and digitizer used for this experiment were the same, it was expected that the data collected with the setup with preamp would have the same accuracy as in A. Laranjeiro's work.

Before the setup with preamp can be used for measurements, a series of measurements were needed to ensure the system performs with good accuracy. Thus, the resolution of the peaks would be the most crucial information. Laranjeiro's work listed the parameter used for the setup with preamp and corresponding resolution [1]. Given that this part would use the same shaping parameters, it would be ideal to use his data as the benchmark for our measurements.

Same as the setup without preamp, during the experiments, the Cs-137 source was placed 15cm away from the detector while the Co-60 source was placed in front of the detector.

Figure 3.7 shows the arrangements of the equipment:

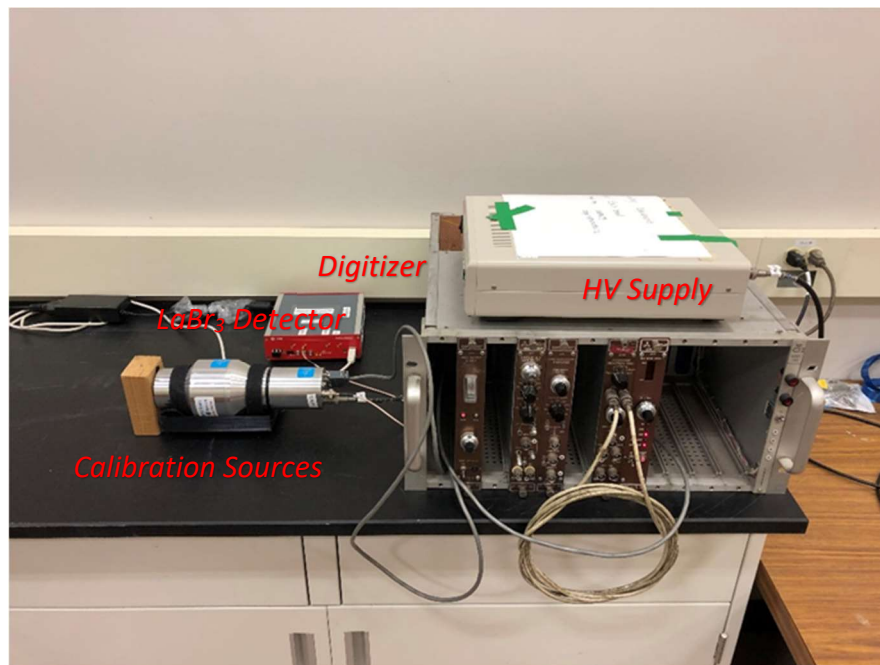


*Figure 3.7: Experiment setup for calibration source measurements (setup with preamp)*

Table 3.5 summarized the results from our work and Mr. Laranjeiro's work. It can be concluded that our measurements had resolutions very close to Laranjeiro's measurements. Thus, the setup with preamp could provide reliable measurements, which can be used for comparison with the setup without preamp.

*Table 3.5: Summary of resolution from our measurements and Laranjeiro's work (setup with preamp)*

	TRT ( $\mu\text{s}$ )	TFT ( $\mu\text{s}$ )	Source	Resolution (%)
This work	0.3	0.5	Cs-137	2.70
Laranjeiro	0.3	0.5	Cs-137	2.68

Table 3.6 shows the lowest energy on the spectrum taken with the setup with preamp. The analysis of the spectrum also showed that the lowest energy that can be covered by setup with preamp is 24.49keV. This energy is much lower than the lower limit for the setup without preamp.

*Table 3.6: Lowest energy on the spectrum (setup with preamp)*

Voltage	Min Channel	Energy (keV)
850V	63	24.49

### **3.5 Determination of the maximum energy on the spectrum (with/without preamp)**

In the previous sections, we have analyzed the lowest energy on the spectrum for the setup with/without preamp. In this section, we determined the spectrum's maximum

energy by performing background measurements. For both setups, a 24-hour background was performed using the optimized shaping parameters. Figure 3.8 and figure 3.9 show the background measurements taken with both setups. Table 3.7 shows the maximum energies covered by both setups.

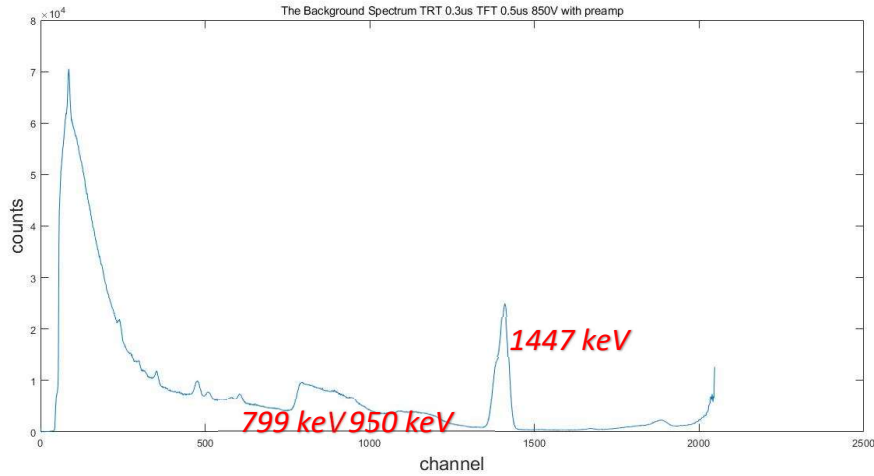


Figure 3.8: Background spectrum obtained with preamp

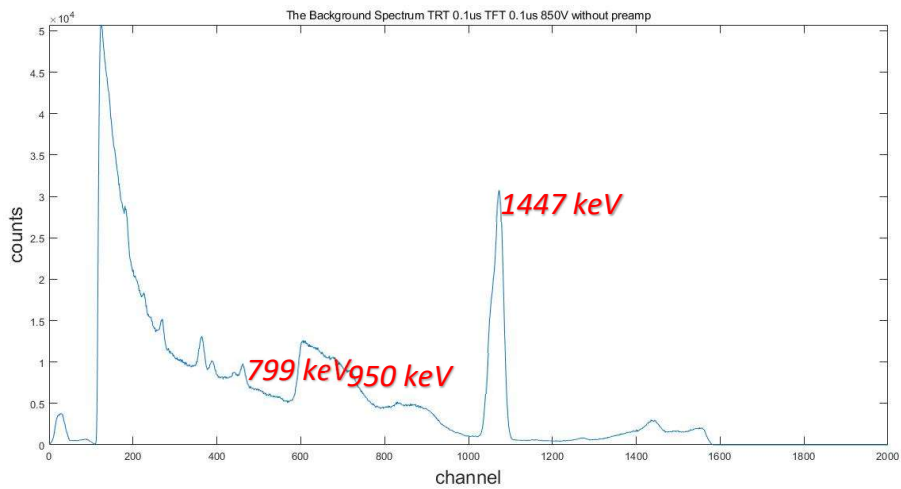


Figure 3.9: Background spectrum obtained without preamp

*Table 3.7: Maximum energy for each setup (based on background spectrum)*

With preamp	Channel number	Max Channel	Max energy (keV)
Yes	2048	2048	2090
No	4096	1584	2152

Based on Laranjeiro's work, the isotope of interest with the highest energy during reactor measurements is Sb-124, with a peak of 1690keV [1]. For both setups, current settings would be able to cover this peak, as well as other peaks of interest.

### 3.6 Optimized Parameters

Based on the experiments, the optimized parameters for the setup without preamp are 0.1 $\mu$ s for the trapezoid rise time, 0.1 $\mu$ s for the trapezoid flat top, and 20lsb for the threshold. With this setting, we were able to obtain spectrum with the best resolution. Also, the dead time is, by comparison, the most ideal. On the other hand, the range of the spectrum can cover all potential peaks of interest in real-life reactor measurements. With all the factors and advantages considered, the settings were optimized.

## **Chapter 4**

### **Calibration Source and Resin Source Measurements**

#### **4.1 Overview**

In previous chapter, we optimized and finalized the shaping parameters for the setup without preamp. Upon the measurements we made, the analysis of the data showed the shaping parameters we chose were the best. However, given the measurements were made at low count rate environments, it is uncertain if the same rule would apply with higher count rate measurements. Thus, we performed more experiments. Also, we performed comparisons between two configurations at various count rate environments.

Hence, in this chapter, we completed both tasks. We first began the experiment by comparing the two setups at low count rate. Then, using the resin Cs-137 sources, we created a higher count rate for measurements for parameters testing and setup comparisons.

#### **4.2 Calibration Sources Measurements (with/without preamp)**

In this section, we performed measurements for the calibration sources. The source arrangements were the same as in the previous chapter: Co-60 source was placed in front

of the detector and the Cs-137 source was placed at 15cm away from the detector. In terms of the shaping parameters, the optimized parameters from chapter 3 were applied.

Table 4.1 shows the measurements taken by different setups. It shows the setups without preamp have both better dead time and resolution. At roughly similar count rates, the setup without preamp has a dead time of 1.74%, which is about 0.4% shorter than the setup with preamp. Although the Cs-137 peak resolution in both setups is not as high as the value given by the manufacturer, the setup without preamp still had better resolution than the old setup.

*Table 4.1 Summary of measurements from calibration sources (with/without preamp) with input count rate around 1800cps*

Without Preamp				
TRT ( $\mu$ s)	TFT ( $\mu$ s)		Resolution (%)	Dead time (%)
0.1	0.1	Cs-137	2.78	1.74
		Co-60	1.83	1.74
			1.81	1.74
With Preamp				
0.3	0.5	Cs-137	3.06	2.10
		Co-60	2.02	2.10
			1.78	2.10

### 4.3 List and Wave Mode in COMPASS Software

The MC<sup>2</sup> software used for signals processing has two modes for data acquisitions: the wave mode and the list mode.

In the wave mode, the input signals are processed, and a portion of the processed waveform are saved in local memory [11]. Thus, the waveform can be observed by using the Oscilloscope mode. This mode is mainly used for shaping parameter adjustments for it can provide real-time waveform information. However, the dead time is higher due to the extra processing, especially during high-count rate measurements. Figure 4.1 shows a sample of the software running in wave mode.



Figure 4.1: Sample of the software running in wave mode

The list mode is different as it only provides the arriving time and the charge of the input signals. In the list mode, no waveform can be observed. As soon as the previous event reaches certain size, the next event is processed. Thus, the processing time is greatly reduced compared with the wave mode. However, in list mode, no histogram can be

made on board, but the list information can be carried into MC<sup>2</sup> software to make spectrums.

In the previous measurements, the COMPASS software was sat in the wave mode for more accessible shaping parameters changing. But to lower the dead time, the list mode would perform much better than the wave mode. Hence, we had to switch the acquisition mode to wave mode. Before such change could be made, we ran several tests to ensure the quality of the spectrum would be stable in this mode. In the measurements below, we used the same calibration source arrangement and performed the measurements with the setup without preamp.

Table 4.2 shows the measurements taken with different mode. The conclusions can be summarized into two main points. Firstly, the resolution remained roughly the same after the switch of the acquisition mode. Secondly, the dead time can be reduced dramatically by using the list mode. After the switch, the dead time changed from 1.64% to 0.22%, which is 13% of the previous value.

*Table 4.2: Summary of measurements from calibration source with different modes (with preamp)*

	TRT ( $\mu$ s)	TFT ( $\mu$ s)		Resolution (%)	Dead time (%)
List Mode	0.1	0.1	Cs-137	2.75	0.22
Wave Mode	0.1	0.1	Cs-137	2.72	1.64

Table 4.3 shows the measurements taken in list mode with both setups.

*Table 4.3: Summary of measurements from calibration source with different setups (list mode)*

	TRT ( $\mu$ s)	TFT ( $\mu$ s)		Resolution (%)	Dead time (%)
With Preamp	0.3	0.5	Cs-137	2.76	0.26
Without Preamp	0.1	0.1	Cs-137	2.75	0.22

List mode showed much better performance during the comparison; thus, list mode was chosen for all following measurements.

#### **4.4 Resin Source Measurements (without preamp)**

##### *4.4.1 Overview*

After using calibration sources for low count rate measurements, the next step was to repeat the exact measurements with a much higher count rate. The goal of this section was to test the impact of using different shaping parameters and their response with different count-rate. In the end, the comparisons between the two setups was performed to prove the setup without preamp would have better dead time even at a higher count rate.

To create various high counts for measurements, we used four Cs-137 resin sources simultaneously. In theory, each resin source would have a much higher activity than the

calibration we used previously. Figure 4.2 shows the source arrangements for the resin sources measurements.



*Figure 4.2: Source arrangement for resin source measurements*

During the experiment, to maximize the count rate, the resin sources were placed around the front face of the detector. Also, the count rate could be easily changed by adding or removing the Cs-137 sources from the detector. It is worth noticing that a Co-60 source was also placed at the front face of the detector.

#### *4.4.2 Measurements with different trapezoid rise time and flat top (without preamp)*

Previous experiments proved the optimized shaping parameters had good preference. However, it was uncertain if the same would apply with a higher count rate. Thus, in this part of the experiment, we tried several sets of parameter settings to find the answer.

During the measurements, all four resin sources were placed around the detector to provide the highest count rate.

Figure 4.3 shows a sample spectrum from the measurements. The Cs-137 peak was clear, but the Co-60 peaks can be barely observed. It was as expected for the Co-60 source used for measurement had very low activity compared with the Cs-137 resin source.

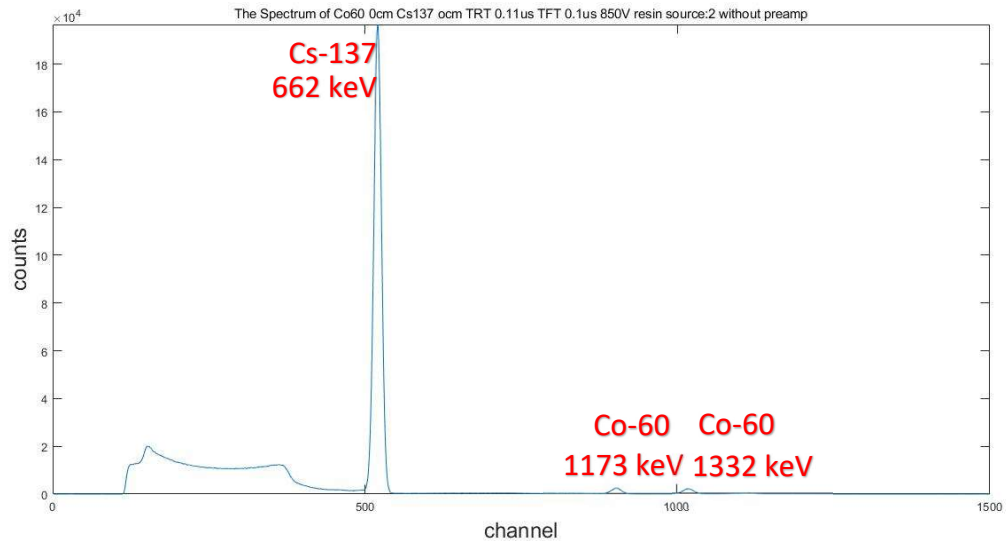


*Figure 4.3: Sample spectrum for the measurements for resin source (without preamp)*

Four slightly different trapezoid rise time and flat top combinations were tested during the measurements. Table 4.4 shows the results taken from the measurements with different shaping parameters. Based on the data collected, the 0.1us and 0.1us combination would provide the ideal dead time. Also, the resolution for the Cs-137 peak is much better, as it is now 2.51%. Although the resolution is still larger than the manufacturer's claim (2.2%), it is an improvement over the previous value, which was

around 2.7%. In conclusion, the optimized parameters (TRT 0.1 $\mu$ s, TFT 0.1 $\mu$ s) are the ideal settings.

*Table 4.4: Summary of measurements with different shaping parameters (without preamp)*

TRT ( $\mu$ s)	TFT ( $\mu$ s)	Threshold (lsb)	Resolution (%)	Dead time (%)
0.09	0.09	20	3.25	5.69
0.10	0.10	20	2.51	5.84
0.12	0.10	20	2.63	6.00
0.15	0.10	20	2.80	6.21

#### *4.4.3 Measurements with different thresholds (without preamp)*

In the previous chapter, we encountered several issues as the spectrum could not cover some of the low-energy regions. In the end, we fixed the issue by changing the threshold setting. In this part, we repeated the measurements with a much higher count rate. The goal was to test whether the 20lsb threshold setting would be ideal even with a higher count rate. Again, we used all four resin sources and the Co-60 source to create a high-count rate environment for measurements.

Table 4.5 summarized the results with different threshold settings. The data shows both 15lsb and 20lsb would enable spectrums to cover the Xe-133 peak (81keV). However, the 20lsb setting would have a lower dead time over the 15lsb setting. Given the lower dead time would always be desired and 20lsb setting could cover all peaks of interest, 20lsb was chosen as the threshold.

*Table 4.5: Summary of measurements with different thresholds (without preamp). TRT and TFT were set at 0.1 $\mu$ s and 0.1 $\mu$ s.*

ICR (cps)	Threshold (lsb)	Lowest Energy (keV)	Resolution (%)	Dead time (%)
$4.16 \times 10^4$	15	35	2.51	5.84
$4.04 \times 10^4$	20	60	2.51	5.68
$3.92 \times 10^4$	25	85	2.50	5.52
$3.79 \times 10^4$	30	110	2.51	5.33

#### *4.4.4 Measurements with different count rates (without preamp)*

After finalizing the parameters settings for the setup without preamp, the following experiments were to make measurements with different high-count rates. The goals contained several parts: Firstly, we tried to investigate how the dead time would change as we increased the count rates. Secondly, we tried to find out how would the resolution change with higher count rates. Finally, the result collected would be used for comparison against the one collected by the setup with preamp. Hence, we would be able to conclude if the dead time can be reduced by using the setup without preamp, at least during the high-count rate measurements.

Unlike the previous sections, a different sets of resin sources were used for measurements. Thus, the highest count rate would be lower. Also, the Cs-137 and Co-60 calibration sources were both used for measurements.

Table 4.6 shows measurements taken with different count rates. It shows the dead time would increase as the count rate increased. Such observations were expected as the dead time is the collection of the processing time for each event. As input count rate increases, the total dead time should also increase. In terms of the resolution, despite the changes in the count rate, the resolution remained largely unchanged which is as expected. It is expected that only with much higher count rates, the resolution would downgrade.

*Table 4.6: Summary of measurements with different count rates (without preamp). TRT and TFT were set at  $0.1\mu\text{s}$  and  $0.1\mu\text{s}$ .*

ICR (cps)	Strong Cs	Peak count rate (cps)	Resolution (%)	Dead time (%)
$1.53 \times 10^3$	0	20.02	2.50	0.22
$2.87 \times 10^3$	1	71.49	2.51	0.42
$1.13 \times 10^4$	2	334.35	2.49	1.63
$1.41 \times 10^4$	3	423.97	2.48	2.02
$2.12 \times 10^4$	4	604.81	2.49	3.02

## 4.5 Resin Source Measurements (with preamp)

### 4.5.1 Overview

The resin source measurements with the setup with preamp contained two steps. In step one, we tried to use a series of measurements to determine if the parameter settings would perform nicely under a higher count rate. In step two, the goal was to use the collected data for comparison. A side-by-side comparison between the measurements from two setups (with/without preamp) would show which setup has lower dead time.

The source arrangements used for measurements were the same as in the previous section in order to achieve better accuracy. The data used for comparison were taken on the same day with the same sources in order to minimize uncertainties.

#### 4.5.2 Measurements with different shaping parameters (with preamp)

Hoping to prove the current setting would perform nicely under the new environment, we tried three sets of shaping parameters in this part. The count rate was maximized using all four Cs-137 resin sources and the Co-60 calibration source. Figure 4.4 shows the sample spectrum for the measurements:

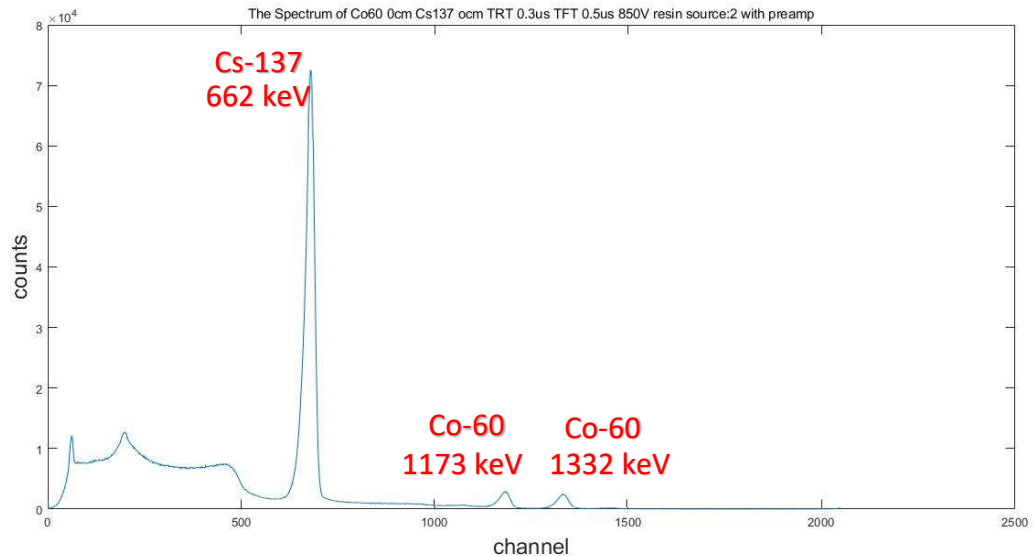


Figure 4.4: Sample spectrum for the measurements for resin source (with preamp)

Table 4.7 summarized the measurements using different shaping parameters. The data suggested that the setting with shorter trapezoid rise time and flat top would have better resolution and dead time. This finding differs from the conclusions drawn from calibration

sources' measurements. The previous experiments showed the ideal setting would be  $0.3\mu\text{s}$  for rise time and  $0.5\mu\text{s}$  for flat top. The trend we observed in calibration sources measurements was that the resolution would decrease as the rise time increased. However, once the rise time reaches  $0.3\mu\text{s}$ , the resolution would increase with the rise time instead.

*Table 4.7: Summary of measurements with different shaping parameters (with preamp). Input count rate is around 25665cps*

TRT ( $\mu\text{s}$ )	TFT ( $\mu\text{s}$ )	Peak count rate (cps)	FWHM (Channel)	Resolution (%)	Dead time (%)
0.1	0.1	574.02	14	3.68	2.50
0.2	0.2	353.25	24	4.69	2.74
0.3	0.3	246.47	33	5.53	3.23
0.3	0.5	185.99	45	6.62	3.73
0.4	0.4	186.16	42	6.37	3.72

A significant difference can be observed if we compare our resolution with Laranjeiro's work, with the shaping parameters the same and the count rate at a similar level. At around 25000cps, Laranjeiro 's data has a resolution of around 2.72%, while our data has a resolution of 6.62% [1]. During the calibration sources measurements, with similar count rate and shaping parameters, our resolution was almost identical to Laranjeiro 's. It is uncertain what may have caused this issue. Thus, we tried to find the cause in the following sections with more measurements.

#### *4.5.3 Measurements with different count rates (with preamp)*

In the previous section, we observed unexpected results as the resolution was much worse than expected. The resolution was very different compared with the data from Laranjeiro's work. Thus, in this section, we tried to approach the issue with several steps.

Firstly, we tried to perform measurements at different count rates. The goal was to find the relation between the count rate and resolution. Secondly, a different preamp power supply was introduced, as the power supply used from previous measurements was not the same model used by Laranjeiro. It is possible that the preamp power supply had certain issues that affected the spectrums' quality.

Regarding the sources, the arrangements were the same as previously described. Both calibration sources and resin sources were used, and the count rates were changed by changing the number of Cs-137 resin sources present. Figure 4.5 shows the spectrum with different count rates.

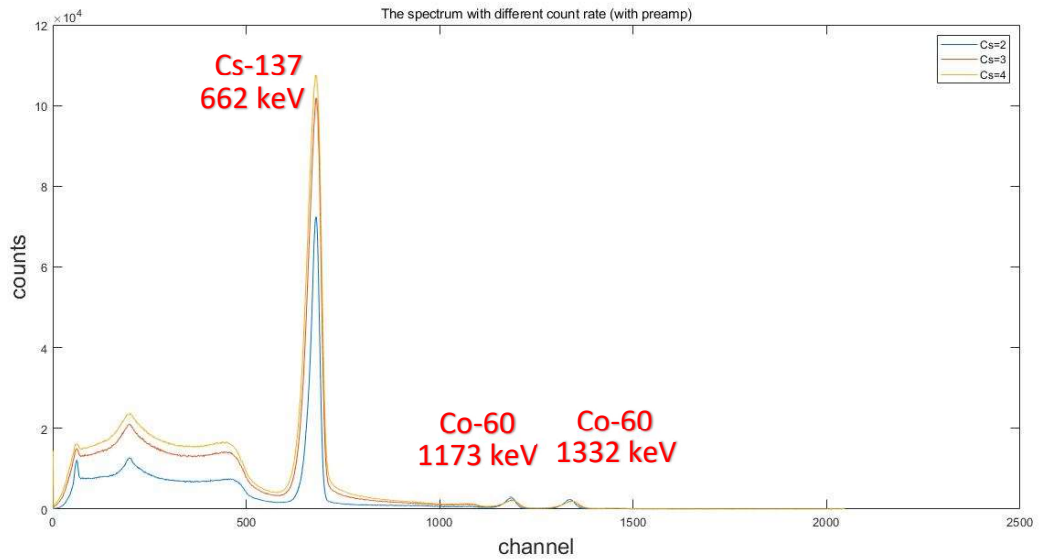


Figure 4.5: Spectrum for the measurements with different rates (with preamp)

Table 4.8 shows the measurements with different count rates. Based on the data collected, the dead time would also increase as the count rate increased. Such is the same pattern observed in similar measurements using the new setup. However, the resolution showed a different trend as the increasing count rates greatly influences the resolution.

Table 4.8: Summary of measurements with different count rates (with preamp). TRT and TFT were set at  $0.3\mu s$  and  $0.5\mu s$ .

ICR (cps)	Resolution (%)	Dead time (%)
$2.06 \times 10^3$	2.75	0.32
$8.54 \times 10^3$	3.41	1.31
$1.12 \times 10^4$	3.77	1.72
$1.37 \times 10^4$	4.32	2.20
$2.36 \times 10^4$	6.48	3.90

Compared with the data from table 4.8, data from measurements without preamp showed the resolution was stable despite the changes in count rates. Laranjeiro 's measurements with preamp also showed a similar trend, as the resolution was stable throughout the experiments [1].

Figure 4.6 shows the relation between resolution and different count rates. The resolution from Laranjeiro 's data only slightly changed when the count rate increased [1]. On the other hand, our resolution experienced a huge increase and changed from 2.75% to 6.48%. It seemed that our setup was more sensitive to the change in the count rate.

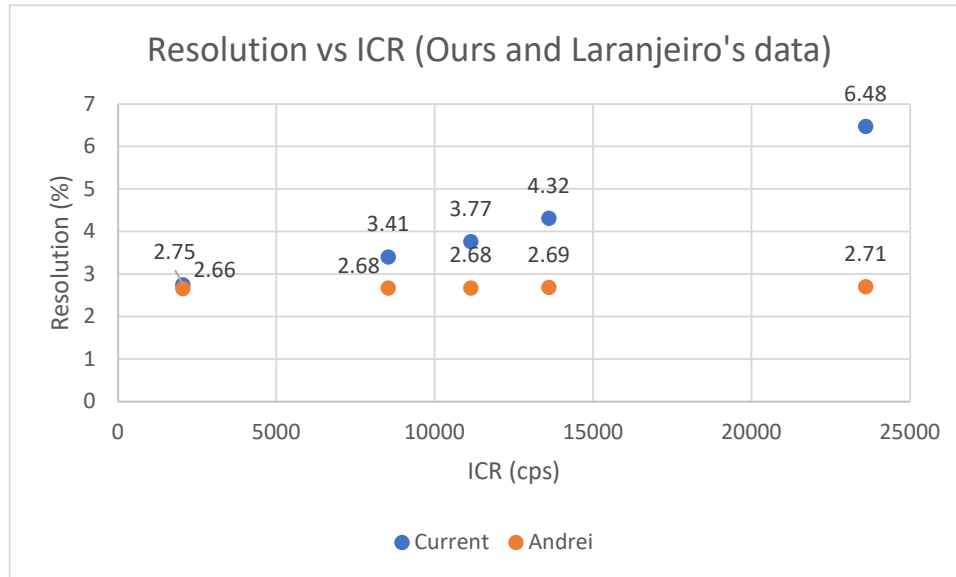


Figure 4.6: Relation between resolution and input count rate (our data and Laranjeiro's data)

As the preamp power supply could be damaged and had unstable output, a new CAEN preamp power supply was used for a series of measurements. The model was the same as the one used by Laranjeiro [1]. Hence, if the problem was caused by a damaged power

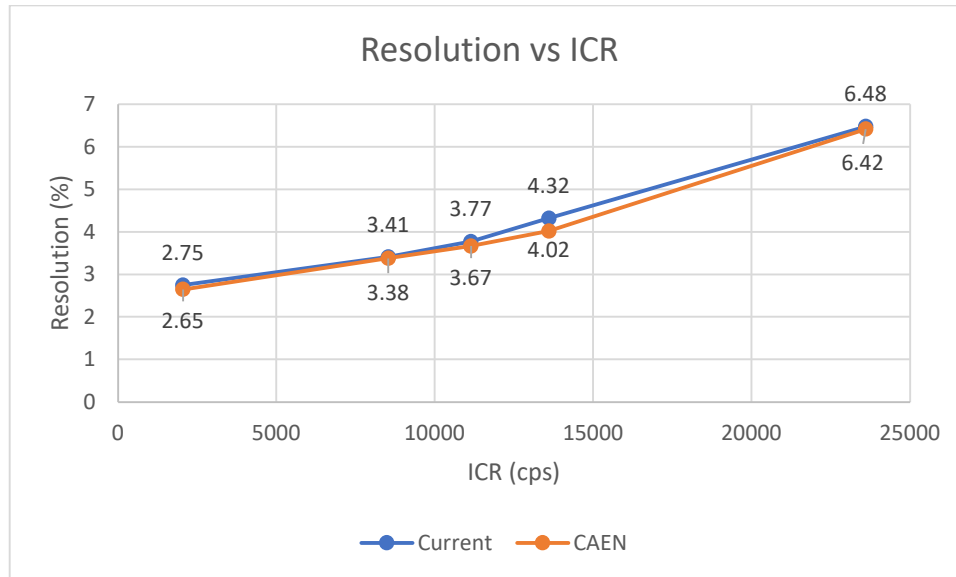
supply, using the new supply should solve the problem. In the following measurements, only the preamp power supply was changed, and other components were kept the same.

Table 4.9 shows the measurements taken with new preamp. The data collected with the CAEN power supply were similar to those collected with the old power supply. The resolution issue remained, despite a different preamp power supply was used.

*Table 4.9: Summary of measurements using CAEN preamp power supply (with preamp). TRT and TFT were set at  $0.3\mu\text{s}$  and  $0.5\mu\text{s}$ .*

ICR (cps)	Strong Cs	Peak count rate (cps)	Resolution (%)	Dead time (%)
$1.86 \times 10^3$	0	14.04	2.65	0.28
$1.15 \times 10^4$	2	122.86	3.67	1.70
$1.38 \times 10^4$	3	175.04	4.02	2.18
$2.56 \times 10^4$	4	185.99	6.42	3.73

Figure 4.7 shows relation between resolution and input count rate with a different preamp power supply. The trend shows the measurements from different power supplies could have similar resolutions. Combined with the fact that at low count rate, we had similar resolutions as Laranjeiro 's data. At this point we concluded the problem may not be a damaged preamp power supply.



*Figure 4.7: Relation between resolution and input count rate (Current preamp power supply and CAEN preamp power supply)*

Given the measurements from the setup without preamp showed good results, the cause of the unexpected issue might be the preamp module attached to the detector.

#### **4.6 Comparison between two setups**

Despite the resolution issue in the measurements with preamp, we still managed to obtain valuable data. We measured the resin sources with two setups (with/without preamp), and the analysis showed good results.

Table 4.10 shows the comparison between the setup with preamp and the one without preamp. Compared with the setup with preamp, the new setup has better dead time at high count rates. As the count rate and total dead time have increased, the difference

between the dead time for the two setups also increased. Hence, the new setup is expected to have even better dead time at higher count rates. The resolution with the new setup is also more stable at high count rates. However, it is yet certain the cause of the resolution issue in the setup with preamp. Hence, we cannot confirm if the new setup would have better resolutions at high count rates.

*Table 4.10: Summary of measurements using two setups (with/without preamp) with input count rate around  $4.2 \times 10^4$  cps*

Preamp	TRT ( $\mu$ s)	TFT ( $\mu$ s)	Peak	Threshold (lsb)	FWHM (Channel)	Resolution (%)	Dead time (%)
Yes	0.3	0.5	Cs-137	40	60	8.49	6.10
No	0.1	0.1	Cs-137	20	7	2.51	5.68

The comparisons above proved that the setup without preamp has better performance at both low count rate and high-count rate. It proved our approach to the dead time problem is on the right track. In the following part of the project, we tried to further increase the count rate to ultra-high and determine how well it performed.

## Chapter 5

### Cs-137 Shephard Sources Measurements

#### 5.1 Overview

In this chapter, we discuss measurements conducted using Shephard source, which created an ultra-high-count rates, in order to stimulate high count rates in power reactor environment. As the main goal was to test if the dead time could be lowered while preserving a good resolution, the high-count rate measurements therefore are the most critical parts of this project.

In the previous sections, we formed several conclusions by using both calibration sources and Cs-137 resin sources. First, the new setup that didn't include preamp can have better dead time. Secondly, the resolution for the new setup was better. However, given these conclusions were formed at a lower count rate measurement, it was uncertain if the same trend would hold at a higher count rate; thus, we designed a series of measurements for testing.

For this part of the project, instead of only having the two setups from the previous sections, a new setup, one included the ion chamber, was introduced. Figure 5.1 and figure 5.2 shows both setups. The ion chamber could provide more accurate dose information than other instruments. The goal was to use the ion chamber for accurate measurements and then use this information to determine if the new setup is reliable.

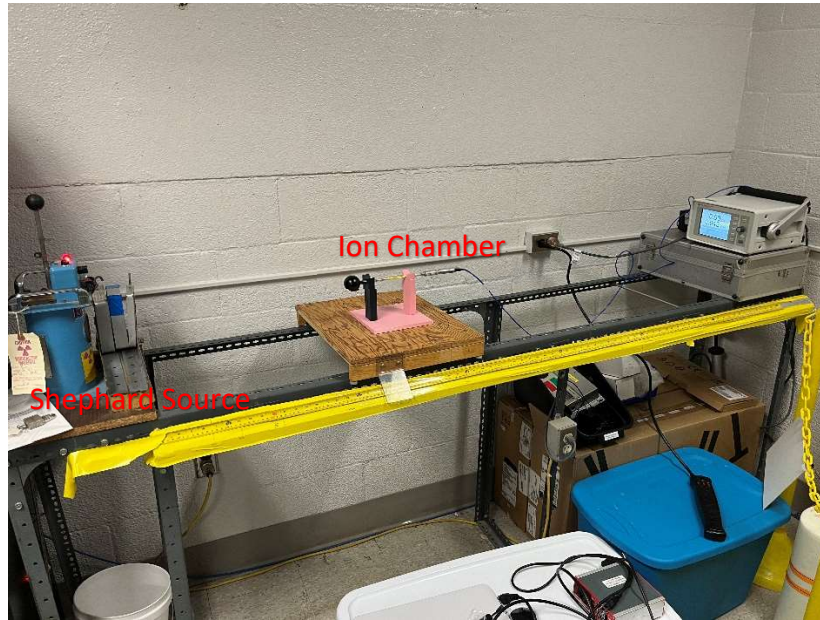


Figure 5.1: Setup for the measurements with ion chamber

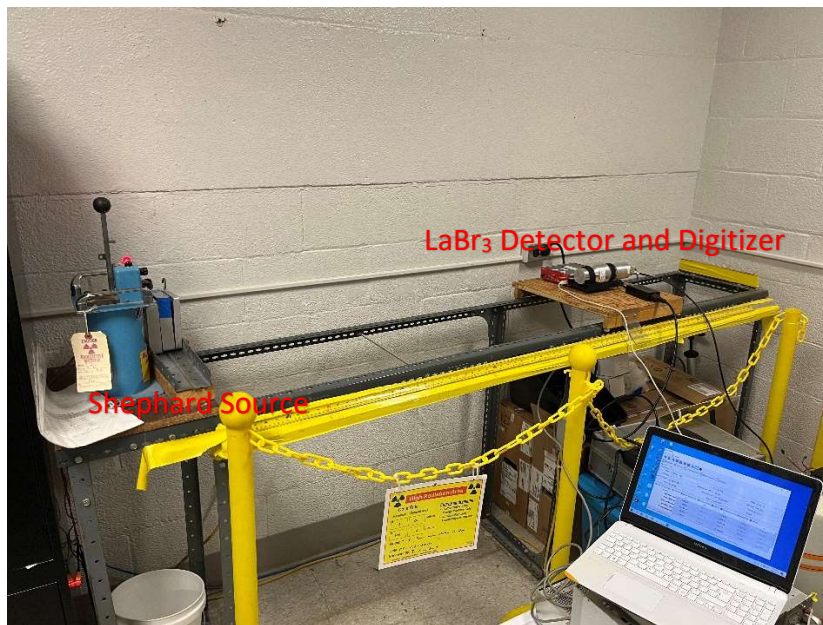


Figure 5.2: Setup for measurements with  $\text{LaBr}_3(\text{Ce})$  detector (with preamp)

The ion chamber or the detector was placed on a moveable platform during the measurements. The meter at the side of the trail made it easier to change source to detector distances. Finally, the front face of the detector is perfectly aligned with the source, as previous research showed angles between the detector and the source would affect the results [1].

The Shephard source used for measurements is a strong Cs-137 source. Hence, only the 662keV gamma line was expected. However, additional gamma peaks may be present in the spectrums due to the presence of other sources and the background radiation.

## **5.2 Measurements with LaBr<sub>3</sub>(Ce) detector (without preamp)**

The new setup's measurements (without preamp) can be divided into three parts. In part one, the goal was to test the dead time and resolution at different count rates. In part two, we tried to find out if we could extend the range of spectrums by changing the voltages. Finally, in the last part, we changed the shaping parameters to investigate if the current shaping parameters are more ideal than the others.

### *5.2.1 Measurements with different input count rate*

In this section, we changed the count rate by changing the source-to-detector distance. Five positions (2m, 1.5m, 1m, 0.5m, and 0.3m) were chosen to provide various count rates. These measurements will be used for comparison in the later sections. In terms of the

settings, both the shaping parameters and voltages were kept the same as the settings from the previous measurements. Figure 5.3 is an example of the spectrum collected:

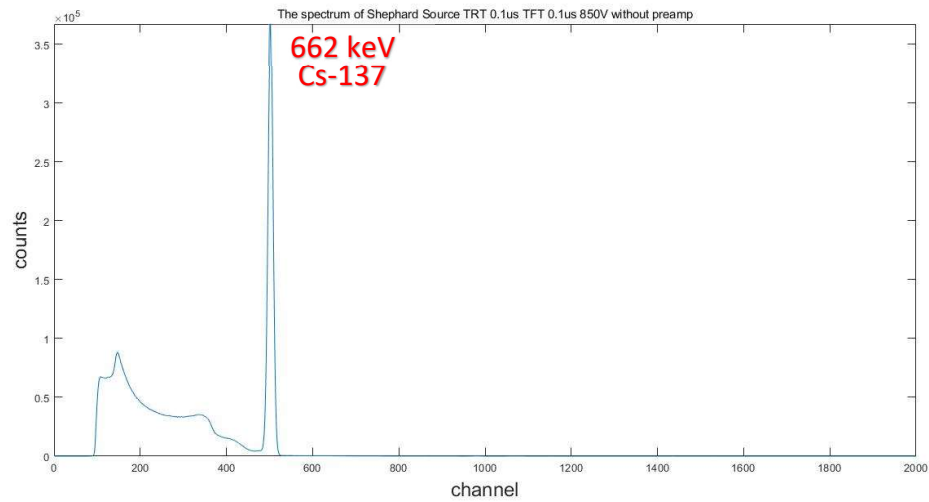


*Figure 5.3: Sample spectrum of the measurements obtained without preamp*

After collecting five sets of data, we plotted and analyzed the spectrum. The results are showed in figure 5.4 and table 5.1. As expected, it can be observed from table 5.1 and figure 5.4 that as the count rate increases, the dead time also increases. The resolution also increased as a result of the increasing count rate. A similar pattern was observed during resin sources measurements

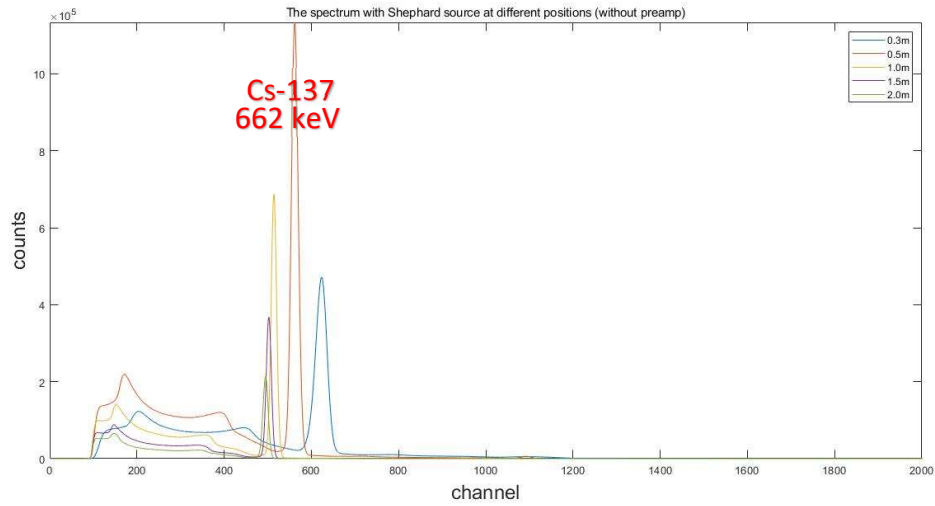


Figure 5.4: Spectrum at various positions (2m, 1.5m, 1m, 0.5m, and 0.3m) acquired without preamp

Table 5.1: Measurements at multiple positions (without preamp). TRT and TFT were set at  $0.1\mu\text{s}$  and  $0.1\mu\text{s}$ , respectively

Position (m)	ICR (cps)	RCR (cps)	Resolution (%)	Dead time (%)
2.0	$4.53 \times 10^4$	$4.52 \times 10^4$	2.42	6.42
1.5	$7.24 \times 10^4$	$7.23 \times 10^4$	2.59	10.07
1.0	$1.46 \times 10^5$	$1.45 \times 10^5$	2.92	19.30
0.5	$5.12 \times 10^5$	$4.95 \times 10^5$	3.20	53.54
0.3	$1.26 \times 10^6$	$1.22 \times 10^6$	4.81	86.23

Table 5.2 shows the comparison between our measurements and the data from Laranjeiro's work. It is worth noticing that at the 0.5m position; the live time count rate is  $4.95 \times 10^5$  cps which is even higher than the highest count rate obtained from the previous work ( $4.8 \times 10^5$  cps) [1]. The dead time at this position also appeared smaller than the

previous research as the dead time changed from 87% to 54% [1]. However, measurements from two research were taken at a different time and with different sources. Hence, this comparison is only for rough testing.

*Table 5.2: Our measurements and Laranjeiro's CANDU measurements*

	Input Count Rate (cps)	Dead Time (%)
Laranjeiro		
Our work	$1.22 \times 10^6$	86.23
Laranjeiro	$4.80 \times 10^5$	87.00
Our work	$5.00 \times 10^5$	53.54
Laranjeiro	$1.10 \times 10^5$	28.00
Our work	$1.40 \times 10^5$	19.30

### *5.2.2 Measurements with different voltages*

During the previous experiments, where measurements were performed with calibration sources, we tried several different HV values to find potential methods to extend the lower boundary of the spectrum. As a result, changing the HV was not the most effective method. However, in this section, we discussed if the same finding would stay at a much higher count rate.

The shaping parameters remained the same throughout the measurements, and the detector was placed at 0.5cm to have a higher count rate. In contrast to the previous experiments, only three voltages were chosen to simplify the measurements.

As high voltages increase, figure 5.5 and Table 5.3 show that more of the low-energy signals would be processed. The dead time was also higher due to the higher count rates.

Similar to the previous experiments with lower activity sources, resolutions would be the lowest at 850V. Also, the dead time at 850V is moderate.

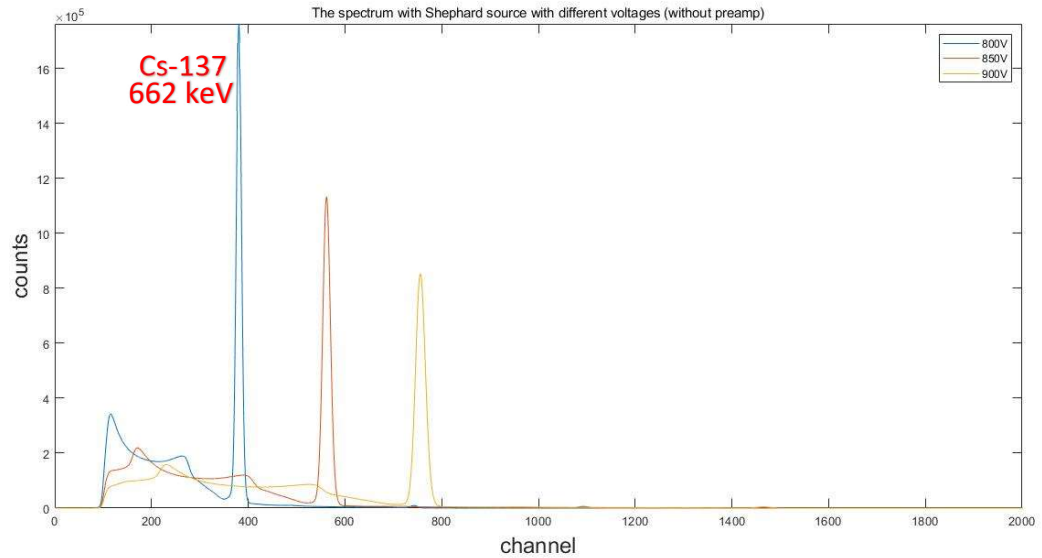


Figure 5.5: Spectrum with different voltages (without preamp)

Table 5.3: Measurements at various voltages (without preamp) TRT and TFT were set at 0.1µs and 0.1µs at 0.5m

Voltage (V)	RCR (cps)	Resolution (%)	Dead time (%)
800	$4.60 \times 10^5$	3.41	49.67
850	$5.12 \times 10^5$	3.21	53.54
900	$5.33 \times 10^5$	3.30	55.05

Analysis of the lower boundary of the spectrums showed the lowest energy available for detection is around 65keV. Such value would be able to cover the 81keV peak (Xe-133), which may present in real-life measurements. The analysis in this section showed the current HV setting is suitable for measurements.

### *5.2.3 Measurements with different shaping parameters*

We tested several different shaping parameters in the final section of Shephard measurements. The goal was to determine if the current setting would still be the ideal setting at a higher count rate. Previous experiments showed the current settings would perform better than other options; however, it may be different at a higher count rate environment.

The main issue would be the pile-up caused by a much higher count rate. As the calibration source experiment showed, higher trapezoid rise time and flat top would generally lead to better resolution. This trend would change at a certain point as settings beyond that point would cause the resolution to increase. The same trend would be expected at a higher count rate, but longer rise time and flat top would also cause more severe pileups. As a result, dead time would be higher, and more counts would be lost. Hence, in this section, we tried two more parameter settings. All the measurements were performed with 850V applied, and detector was placed 0.5m away from the source.

Figure 5.6 shows spectrums for all three measurements. Table 5.4 shows the dead time increased with higher rise time and flat top settings. This increase was to be expected as the rise time, and the flat top are the main contributors to the dead time. The resolution also increased with higher rise time. However, this would not change our choice of shaping parameters.

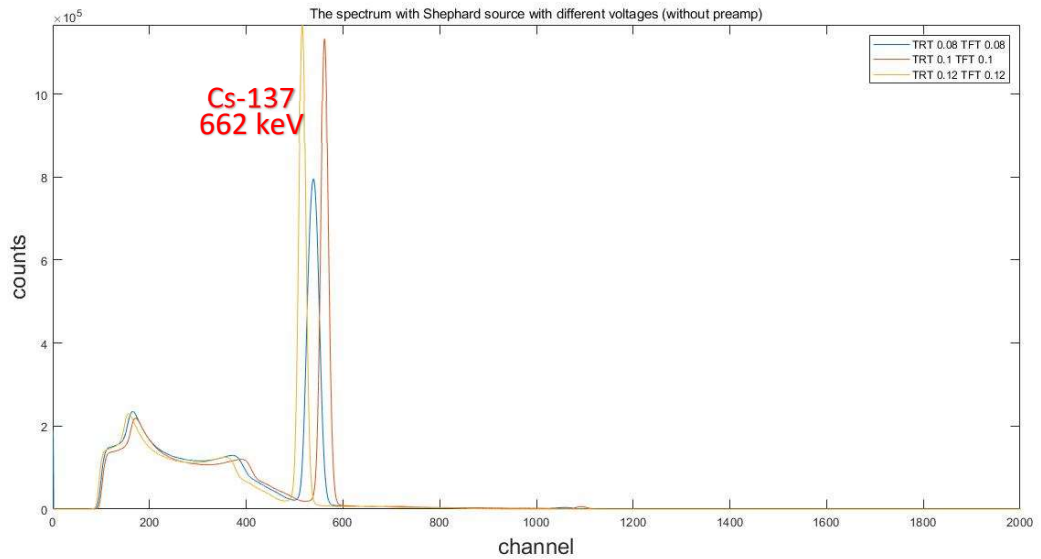


Figure 5.6: Spectrum with different shaping parameters (without preamp)

Table 5.4: Measurements with different shaping parameters (without preamp) at 0.5m

TRT ( $\mu\text{s}$ )	TFT ( $\mu\text{s}$ )	RCR (cps)	Resolution (%)	Dead time (%)
0.08	0.08	$5.07 \times 10^5$	5.03	51.34
0.10	0.10	$5.12 \times 10^5$	3.50	53.54
0.12	0.12	$5.08 \times 10^5$	3.49	54.83

Firstly, the differences between the two resolutions are relatively small. Secondly, the difference between the dead time, on the other hands, is larger. Also, this difference would be much higher with ultra-high-count rate measurements. As the main goal for this project is to minimize the dead time, parameter setting with lower dead time would always be desired. Finally, the 0.12 $\mu\text{s}$  rise time setting has a smaller range. The spectrum's lowest available energy is larger than the one with setting we used. Although it would still

be able to cover the isotopes of interest, spectrum which can cover lower energy would be more desirable.

### **5.3 Measurements with LaBr<sub>3</sub>(Ce) detector (with preamp)**

To investigate whether the setup without preamp would have lower dead time, comparisons between the setups would be needed. Thus, in this section, we performed similar measurements on the Shephard source with the older setup (with preamp).

The structure of the experiment was similar to the one with the new setup. Different count rates, HV, and shaping parameters were chosen for measurements. Data was collected for analysis which focused on dead time and resolution. To ensure better accuracy, measurements with preamp were performed on the same day as the previous experiments.

The arrangement of the detector was the same as in the previous experiment. The center of the front face of the detector was aligned with the center of the Shephard source. Several different source-to-detector distances were chosen to create different count rates.

#### *5.3.1 Measurements with different input count rates*

In this section, HV applied at the detector were kept the same. The shaping parameters used for this experiment were the same as those used in other preamp experiments.

Figure 5.7 shows some interesting results. Unlike measurements with lower activity sources, measurements with Shephard showed much broader peaks. Given that the resolution was calculated using FWHM/peak center, this would lead to a larger resolution. A similar trend was observed during the measurements with Cs-137 resin sources; thus, the larger resolution may be caused by the much higher count rate. However, more issues arose after we had further increased the count rate.

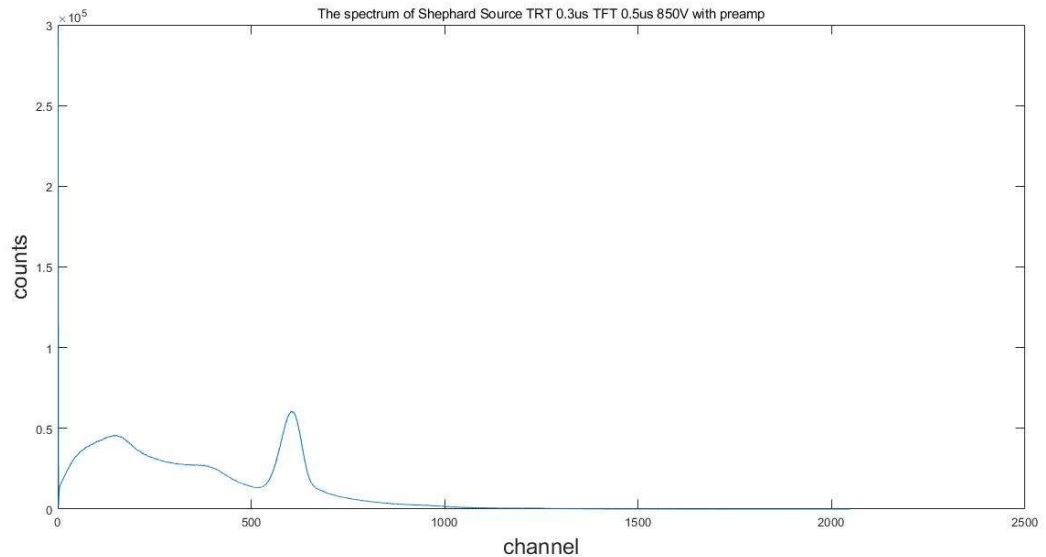


*Figure 5.7: Sample spectrum of the measurements for the setup with preamp*

During the measurements, five different positions were chosen (2m, 1.5m, 1m, 0.5m, and 0.3m). Figure 5.8 shows the collected spectrums, however, only three measurements were analyzed. The problem was the unrecognizable spectrums at an ultra-high-count rate. In figure 5.8, for almost all counts were located at channel 0, we changed the scale

of the spectrum to include only part of the counts at channel 0 in order to see the Cs-137 gamma peak. As in reality, the counts were around  $1.9 \times 10^6$  at 0 channel for 1m position.

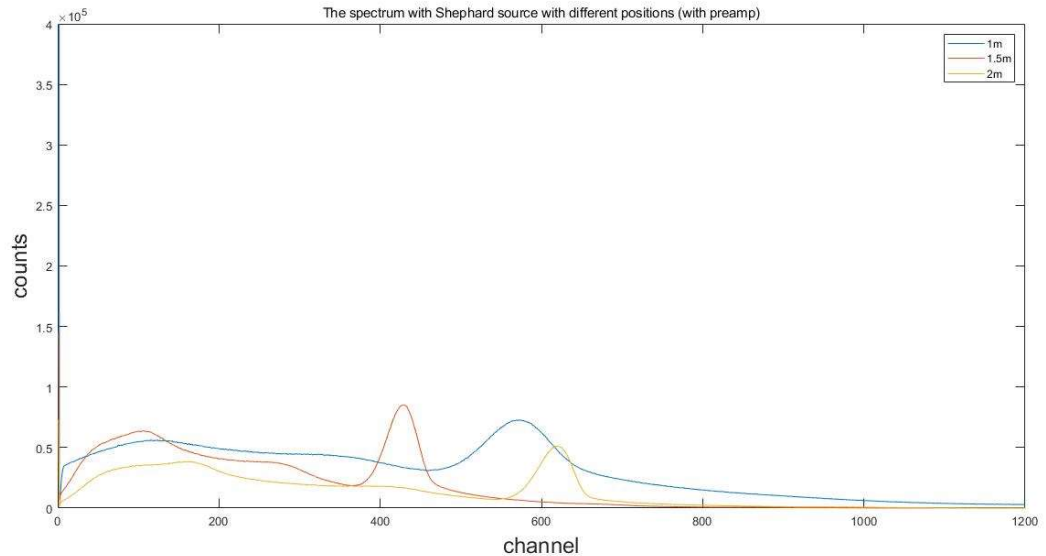


*Figure 5.8: Spectrum at a different position (with preamp)*

Figure 5.9 shows the spectrum taken at the 1m position, with a much higher count rate. As we can see from the spectrum, the Cs-137 peak is becoming harder to identify compared with the previous spectrums, where the count rates were much lower. Most counts have located around 0-10 channels, so they were not properly processed. Spectrums became much worse at 0.5m, and 0.3m positions as the peaks almost disappeared, and the majority of the counts were located at the low channel. Again, we changed the scale of the spectrum for easier peak observation. In reality, the counts were around  $1.9 \times 10^6$  at 0 channel.

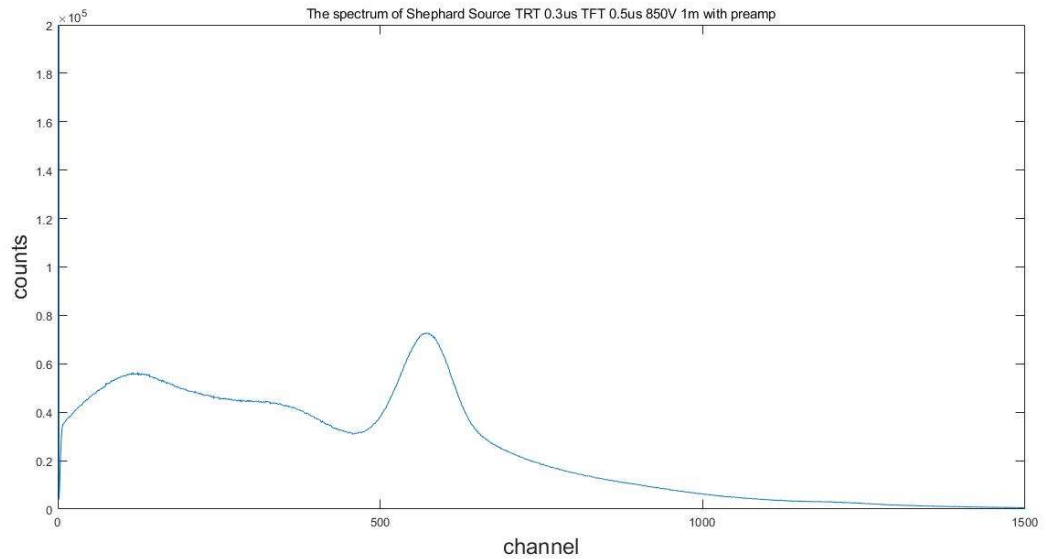


*Figure 5.9: Sample spectrum at 1m position (with preamp)*

The issue in the spectrums showed certain issues exist in the system. Due to the low resolution and poorly made spectrums, the dead time information collected could not be used for comparison. Until the issue has been fixed, there would be no reason to perform any form of comparison with these data.

It is worth noticing that both spectrums and data from Laranjeiro's work showed no issue during similar high-count rate measurements [1]. There were no significant resolution issues. Most importantly, clear peaks can be observed, and counts are located at expected locations. The equipment and shaping parameters used for the measurements were the same as those used in Laranjeiro's work. Thus, the priority was to find the cause of this issue.

The first step was to test the detector with calibration sources, as the detector or the preamp module could be damaged. Testing measurements were performed with the calibration sources before the Shephard measurements. The results were as expected and showed no noticeable difference from previous measurements. Also, two sets of measurements were made with calibration sources and setup with preamp after the Shephard measurements.

Figure 5.10 shows measurements with calibration sources showed no changes. Both Cs-137 and Co-60 peaks were clear, and the resolutions were the same as in the previous experiments. Dead time and output count rate were within expectations.

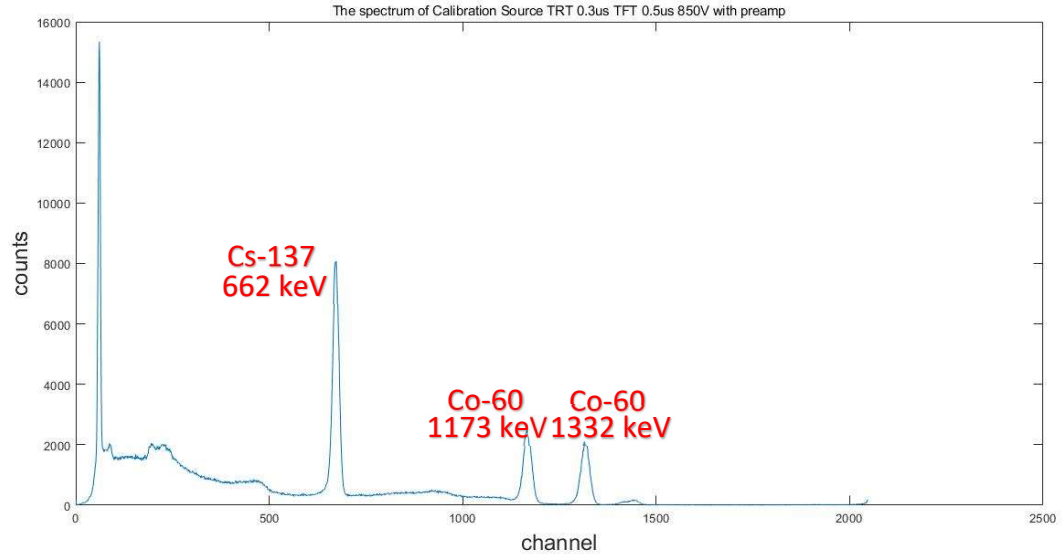


*Figure 5.10: Measurements with calibration sources (with preamp)*

Considering the measurements made earlier that day with the setup without preamp did not show any strange results, the cause of the problem would not be the detector. Thus,

the issue may be caused by the preamp or the preamp power supply. Hence, different voltages and shaping parameters may solve this problem.

### *5.3.2 Measurements with different voltages*

Two voltages, the HV and the voltage applied on the preamp, were used for the setup with preamp. Both voltages would have various impacts on signal processing. Thus, in this section, we tried to change the voltage and determine if this method could solve the problem.

The first approach would be to change the preamp power supply. As the voltage applied at the preamp would determine the maximum height of the signal, this would limit the system's performance, especially at ultra-high-count rate measurements. The main reason would be as the count rate increase; the pile-up would also increase to a point where the previous signal would reach the maximum voltage, thus stopping the next signal from being processed.

A different CAEN preamp power supply was borrowed from another research group for testing. A series of measurements were made using the new power supply while keeping the shaping parameters and HV constant.

Figure 5.11 shows results. In reality, the counts were around  $1.9 \times 10^6$  at 0 channel. Thus, the cause would not be a failed preamp power supply.

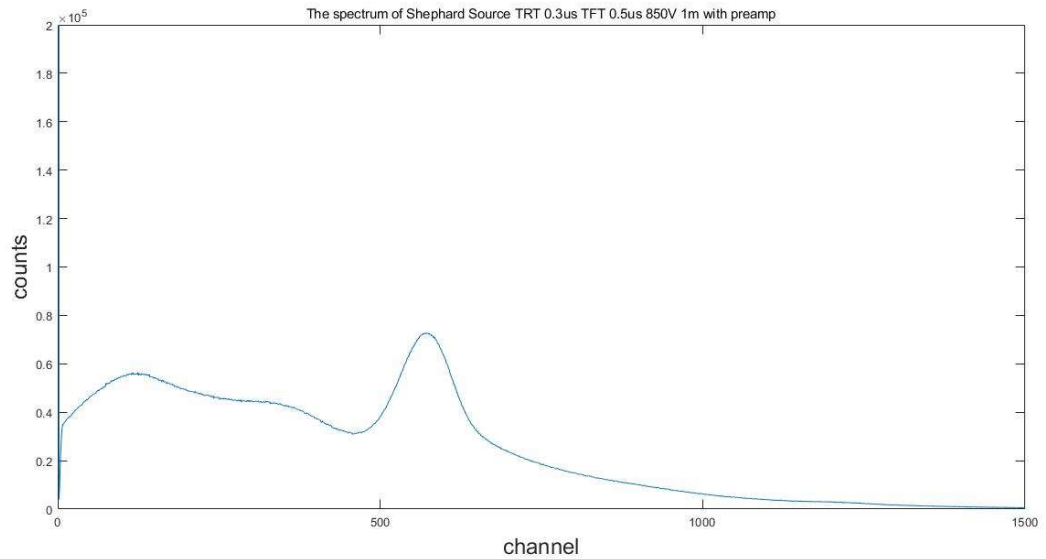


Figure 5.11: Sample spectrum at 1m position with new preamp power supply (with preamp)

The next step was to change the HV applied to the detector. The original goal was to test the setup with preamp's response to different HV.

Theoretically, higher HV should affect the performance of the PMT, as the signal output should increase exponential with the HV [7]. Thus, changing the HV should have very little effect on the problem. To investigate the effects of HV on the setup with preamp, a series of measurements were made with three HV values at the 1.5m position.

As expected, lower HV would mean fewer counts to be processed. On the other hand, a lower count rate also improved the resolution. Figure 5.12 shows the spectrums taken with different HV value. Combining the result from figure 5.12 and figure 5.8, it seems that the system can handle a relatively lower count rate. However, at the ultra-high-count

rate, the detector would be overwhelmed. Lots of signals would not be processed, and the spectrums' accuracy would be lowered.

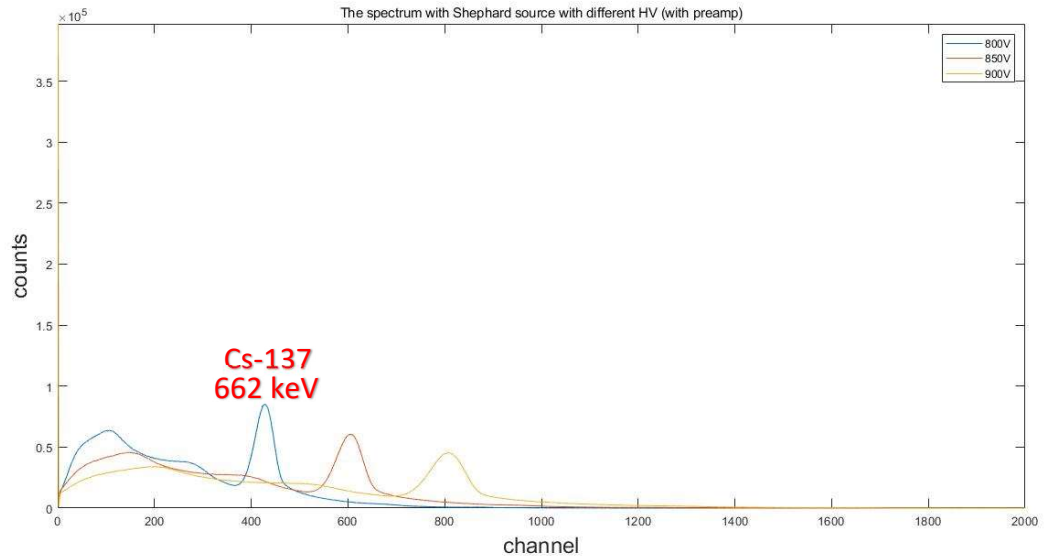


Figure 5.12: Spectrum collected with different voltages settings at 1.5m (with preamp)

### 5.3.3 Measurements with different shaping parameters

In this section, different shaping parameters were used to investigate their effects on the spectrum. Previous experiments on the finding for the ideal parameter settings showed the settings used by Laranjeiro were the ideal setting during low count rate measurements. It was uncertain if the same rule applied to an ultra-high count rate environment.

Three sets of trapezoid rise time and flat top were chosen for measurements. During all three measurements, the detector was placed 1.5m away from the Shephard source, and the HV was kept at 850V.

Figure 5.13 shows lower trapezoid time, and the flat top had the best resolution. It is different from similar measurements made with lower activity sources. One possible explanation would be the lower rise time, and the flat top would decrease the processing time needed for one event, thus, allowing for more counts to be processed at a given time. However, this may not be the conclusion as it is not yet certain if preamp module attached was damaged.

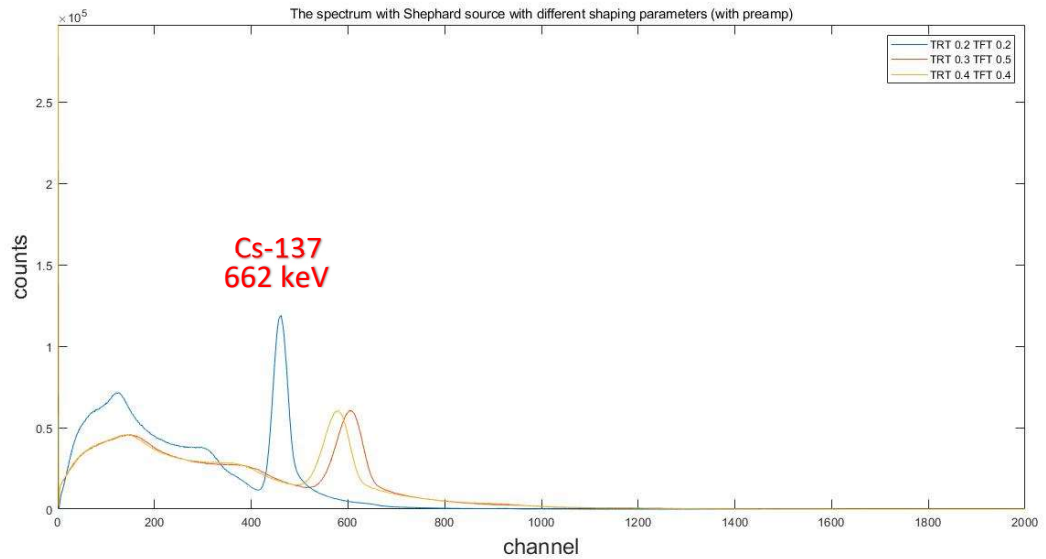


*Figure 5.13: Spectrum with different Shaping Parameters at 1.5m (with preamp)*

From all the measurements with preamp, it can be concluded that our setup with preamp could not handle ultra-high count rate measurements for unknown reasons. The low dead time and the large number of counts located at the low channel during the ultra-high-count rate measurements also suggested not all counts were processed. As the count rate reaches a certain point, the system would stop processing for an unknown reason.

In future research, the investigation of this issue should focus on two aspects. Firstly, a preamp power supply capable of providing higher voltage should be tested. Secondly, a new preamp module should be used for similar measurements. The comparison between different preamp modules may prove if the module current in use was damaged.

#### **5.4 Ion chamber measurements**

During the Shephard source measurements, we also used ion chamber to measure the dose rate. The model we used is a TK30 Type 32005 ion chamber made by PTW-Freiburg [16]. However, the ion chamber we used was newly arrived and had not been fully tested. To avoid possible errors, we also used a Bot P200 dose meter for measurements. The idea was that, although the accuracy of the P200 is less than the ion chamber, the results should be close. Thus, if the results from ion chamber and P200 are close, then the results from ion chamber can be reliable.

The actual analysis of the data from the ion chamber and P200 was slightly complicated as the results were recorded in different units. The ion chamber used  $\mu\text{Gy/s}$  while the P200 recorded in  $\text{mrem/h}$ . After simple conversion, we could obtain the results with same units.

The  $\mu\text{Gy/s}$  measured by the ion chamber was absorbed dose. Given the radiation measured was gamma-ray, the radiation weighting factor would be 1. Thus, we obtained

the effective doses. With the tissue weighting factor to be 1, considering the whole body, we could then calculate the effective dose. The example of such calculation is as follows:

$$D_{ab} = 0.084 \left[ \frac{\mu Gy}{s} \right] \quad (5.1)$$

$$D_{equ} = D_{ab} \times 1 = 0.084 \left[ \frac{\mu Sv}{s} \right] \quad (5.2)$$

$$D_{eff} = D_{equ} \times 1 = 0.084 \left[ \frac{\mu Sv}{s} \right] = 30.24 \left[ \frac{mrem}{h} \right] \quad (5.3)$$

By performing the conversion to all ion chamber measurements, we obtained the results with the same unit as the measurements from P200. Table 5.5 shows results from different meters had similar results. In addition to that, all results obeyed the inverse square law. Thus, the ion chamber measurements can be used for comparison against the measurements from the LaBr<sub>3</sub>(Ce) detector.

*Table 5.5: Measurements from ion chamber and P200*

Distance (m)	Ion Chamber (mrem/h)	P200 (mrem/h)
0.5	30.2	31.2
1.0	7.6	8.5
1.5	3.2	3.7
2.0	1.8	2.3

## 5.5 Comparing the ion chamber and detector (without preamp) measurements

Different from the measurements with the ion chamber, results from measurements with LaBr<sub>3</sub>(Ce) detector were in different units. Given the COMPASS would record the measurements in counts instead of dose or dose rate, a series of calculations would be needed to convert the results into dose rate.

The first step was to find the live time net peak count rate for the Cs-137 peak in each spectrum. It can be done by using the analysis function in the COMPASS software and the live time recorded. The equation is as followed, where the  $C_p$  is the net peak count rate,  $A_{net}$  is peak area under the Cs-137 peak and  $t_L$  is the live time.

$$C_p = \frac{A_{net}}{t_L} [cps] \quad (5.4)$$

The next component to be calculated was the energy response,  $\epsilon_\phi$ , which can be found by using the MCNP coding. The idea was to divide the peak area by the fluence to obtain the response which would be in cm<sup>2</sup>, with both peak areas and fluence information to be obtained through the MCNP. The energy of the source was chosen to be 662keV to represent the Cs-137 source. In this part, we obtained similar results as the one from the previous work [1].

With both net peak count rate and energy response, the fluence rate can be found by the following equation, where the  $\phi(E_\gamma)$  represent the fluence rate of the specific energy, in this case it was 662keV:

$$\Phi(E_\gamma) = \frac{C_p}{\varepsilon_\phi} [cm^{-2}s^{-1}] \quad (5.5)$$

With equation above, we managed to convert the measurements with the LaBr<sub>3</sub>(Ce) detector into fluence rate. Finally, by using the conversion factor from ICRP 116 table A.1, we obtained the dose rate in mrem/h.

Table 5.6 shows both sets of dose rates are close. Similar to the ion chamber measurements, calculated results also show as the distance increase the dose rate decrease. The difference between two sets of measurements could be caused by various factors. For example, the distance between the detector and Shephard source could be slightly different during the measurements. Also, the case outside the LaBr<sub>3</sub>(Ce) crystal may interfere with the measurements and contribute to the inaccuracy. In conclusion, the data showed the LaBr<sub>3</sub>(Ce) detector without preamp setup can obtain reliable results despite the certain inaccuracy presented.

*Table 5.6: Dose rate from both ion chamber measurements and calculation*

Distance (m)	0.5	1.0	1.5	2.0
Calculated Dose Rate (mrem/h)	33.9	7.7	3.7	2.0
Ion chamber measurements (mrem/h)	30.2	7.6	3.2	1.8

## Chapter 6

### Conclusion

This research aims to solve the large dead time during the ultra-high count rate gamma-ray spectrometry. Thus, the preamp was removed from the system to reduce the processing time of each event. The setup, which is based on the one used by previous research, consists of several components, including a  $\text{LaBr}_3(\text{Ce})$  detector, a HV power supply, a digital pulse processing system, and the data collection laptop. Measurements were made using the modified setup with calibration sources to find the ideal shaping parameters.

Based on the optimization for the new setups, a series of side-by-side comparisons were made between the setup with preamp and the setup without preamp at various count rates. The analysis focused on the resolution and dead time was made for each measurement. Both Cs-137 and Co-60 calibration sources were used to create a low count rate environment. With ICR at  $1.81 \times 10^3 \text{cps}$ , dead time from the setup with preamp is 0.26% which is larger than the one without preamp, which is 0.22%. At the median count rate created by Cs-137 resin sources, with ICR around  $4.2 \times 10^4 \text{cps}$ , setup with preamp also has a larger dead time (6.10%) compared with the setup without preamp (5.68%). Regarding the ultra-high count rate environment created by the Shephard source, the comparisons were troubled as the setup with preamp was unable to provide useful results. However,

the comparison between our measurements and the one from the previous research shows promising results as the dead time change from 87.00% (with preamp) to 53.54% (without preamp) at ICR around  $4.90 \times 10^5$  [1].

Thus, it can be concluded the large dead time at ultra-high count rate measurements can be reduced by removing the preamp from the setup. Also, further improvements could be made in several aspects. First of all, the cause for the performance issue of the preamp module at an ultra-high-count rate is currently unknown. Future work could focus on investigating the potential cause of such issue.

## Reference

- [1] Andre Laranjeiro. The Characterization and Optimization of a LaBr<sub>3</sub>(Ce) Spectroscopy System for High-rate Spectrometry at CANDU Reactors. Master thesis. 2018.
- [2] Cooper, R.J. et al. A prototype High Purity Germanium detector for high resolution gamma-ray spectroscopy at high count rates. Nuclear Instruments and Methods in Physics Research. 2015.
- [3] Löher, B., et al. High-count rate  $\gamma$ -ray spectroscopy with LaBr<sub>3</sub>(Ce): Ce scintillation detectors. Nuclear Instruments and Methods in Physics Research. 2012.
- [4] Nocente, M., et al. High-Resolution Gamma Ray Spectroscopy at MHz Counting Rates with LaBr<sub>3</sub>(Ce) Scintillators for Fusion Plasma Applications. IEEE Transactions on Nuclear Science. 2013.
- [5] G.F. Knoll. Radiation Detection and Measurement - 3rd Ed (Chapter 16-18). John Wiley & Sons. 1999.
- [6] James, E.T. Atoms Radiation, and Radiation Protection (Chapter 10). Wiley-Vch. 2007.
- [7] G. Gilmore, et al. Practical Gamma-Ray Spectrometry. John Wiley & Sons (Chapter 4 and 10). 1995.
- [8] Lanthanum Bromide Scintillators Performance Summary. Saint-Gobain. 2021.
- [9] Lanthanum Bromide and Enhanced Lanthanum Bromide. Saint-Gobain. 2018.

- [10] Structure of the LaBr<sub>3</sub>(Ce) detector. Saint-Gobain. 2011.
- [11] User Manual UM3246 DT5724. CAEN. 2017.
- [12] Manual for 724 Digitizer Family. CAEN. 2019.
- [13] CoMPASS Quick Start. CAEN. 2021.
- [14] Guide GD2080 – Introduction to Digitizer. CAEN. 2014.
- [15] Manual for High Voltage Power Supply. HAMAMATSU. 2021.
- [16] User Manual for Spherical Chamber TK30 Type 32005. PTWFREIBURG. 2017.
- [17] ICRP Publication 116. International Commission on Radiological Protection (ICRP). 2010.
- [18] Christopher J Werner. et al. MCNP User's Manual Code Version 6.2. Los Alamos National Laboratory. 2017.
- [19] J. J. Bevelacqua. Basic Health Physics: Problems and Solutions (Chapter 1). Wiley-Vch. 2010.
- [20] J. Atanackovic, et al. Evaluation of Eye Lens Dosimetry at CANDU Power Plants. Ontario Power Generation. 2018.
- [21] The Ontario Energy Report. Bruce Power. 2020.